Bismuth in Radical Chemistry & Catalysis

汇报人：孙矢劲

导师：张俊良 教授

杨俊锋 青年研究员

2025年11月21日

目录

目录

1. 前言

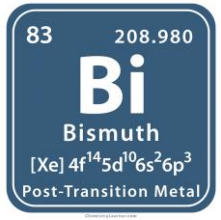

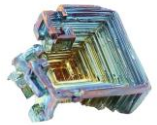

// the **heaviest stable** element
// **remarkably low toxicity** for a heavy metal
// most important synthetic application:
the SOHIO process:
(Standard Oil Company of Ohio)

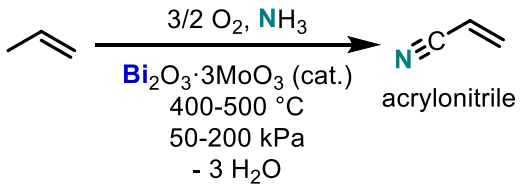

Bi: [Xe] $4f^{14}$ $5d^{10}$ **$6s^2$ $6p^3$** ← outermost electrons

inert pair effect

⇨ various valences: $Bi^{I/II/\mathbf{III}/IV/V}$
where $Bi^{\mathbf{III}}$ is the most dominant

a) www.acs.org/content/dam/acsorg/education/whatischemistry/landmarks/acrylonitrile/sohio-acrylonitrile- process-commemorative-booklet-1996.pdf ;
b) R. K. Grasselli, *Catal. Today* **1999**, *49*, 141–153.

1. 前言

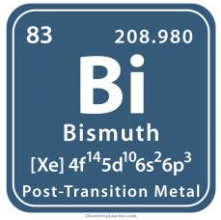

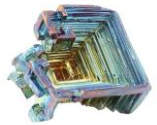

// the **heaviest stable** element
// **remarkably low toxicity** for a heavy metal
// most important synthetic application: **the SOHIO process**: (Standard Oil Company of Ohio)

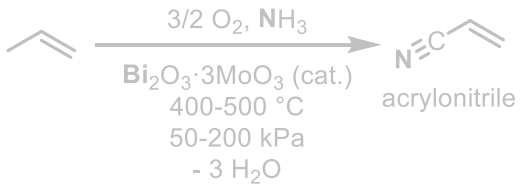

Bi: [Xe] $4f^{14}$ $5d^{10}$ **$6s^2$ $6p^3$** ← outermost electrons

inert pair effect

⇨ various valences: $Bi^{I/II/\mathbf{III}/IV/V}$ where Bi^{III} is the most dominant

Bi^{III}: [Xe] $4f^{14}$ $5d^{10}6s^2$

lanthanide contraction

⇨ Bi^{III} is a potent **soft** Lewis acid

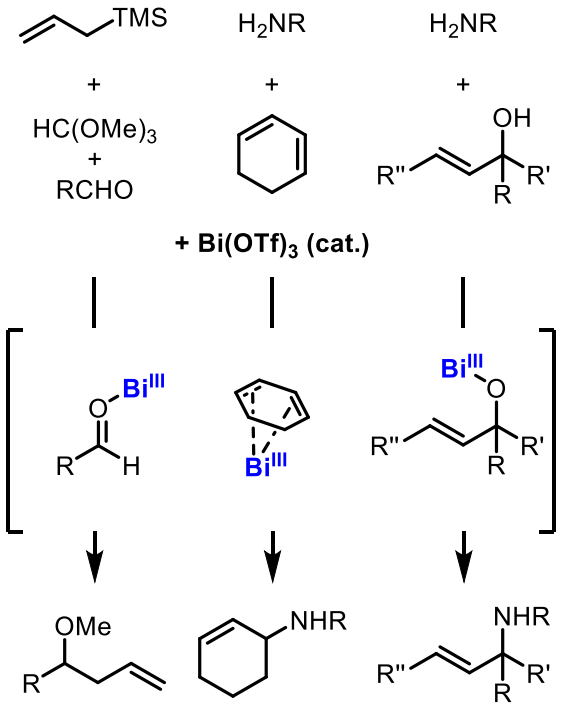

a) R. S. Mohan et al. *J. Org. Chem.* **2005**, *70*, 2091-2096;
b) M. Shibasaki et al. *J. Am. Chem. Soc.* **2006**, *128*, 1611-1614;
c) M. Shibasaki et al. *Angew. Chem. Int. Ed.* **2007**, *46*, 409-413.

1. 前言

83 208.980
Bi
Bismuth
[Xe] $4f^{14}5d^{10}6s^26p^3$
Post-Transition Metal

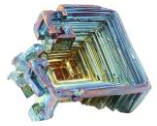

// the **heaviest stable** element
// **remarkably low toxicity** for a heavy metal
// most important synthetic application: **the SOHIO process**: (Standard Oil Company of Ohio)

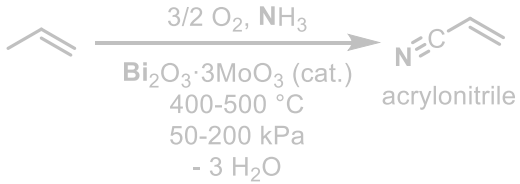

Bi: [Xe] $4f^{14}$ $5d^{10}$ **$6s^2$ $6p^3$** ← outermost electrons

inert pair effect

⇨ various valences: $Bi^{I/II/\mathbf{III}/IV/V}$
where Bi^{III} is the most dominant

Bi^{III}: [Xe] $4f^{14}$ $5d^{10}6s^2$

lanthanide contraction

⇨ Bi^{III} is a potent **soft** Lewis acid

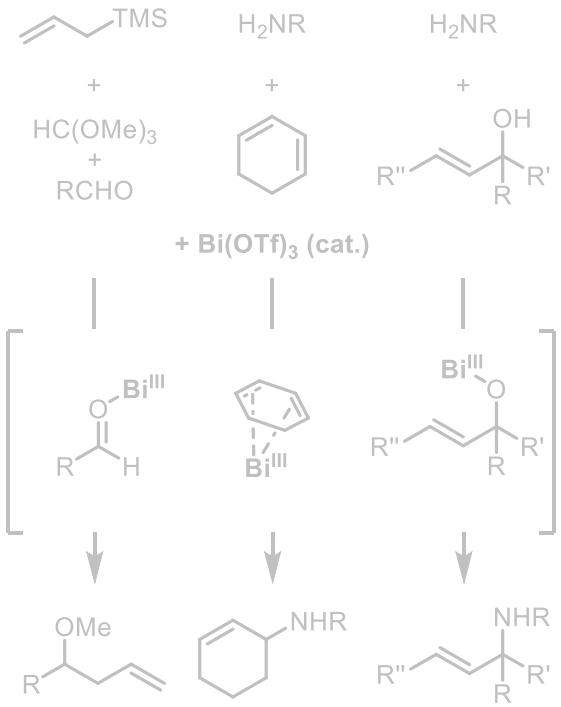

Polar bismuth redox catalysis:
2019 - present

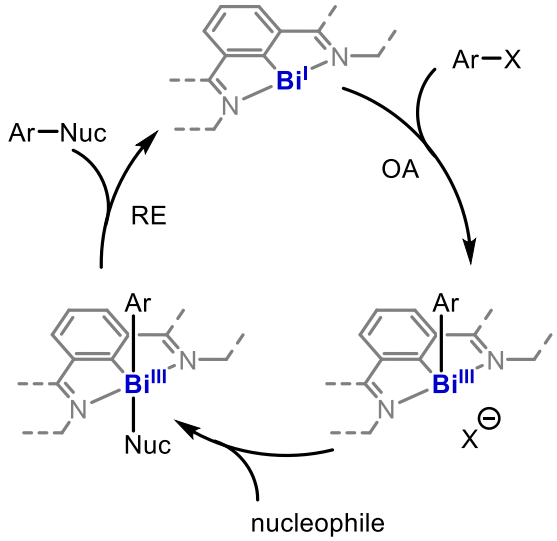

low-valent polar Bi-redox catalysis

Introduced by
Dr. Jun-Xiong He (2022.10)

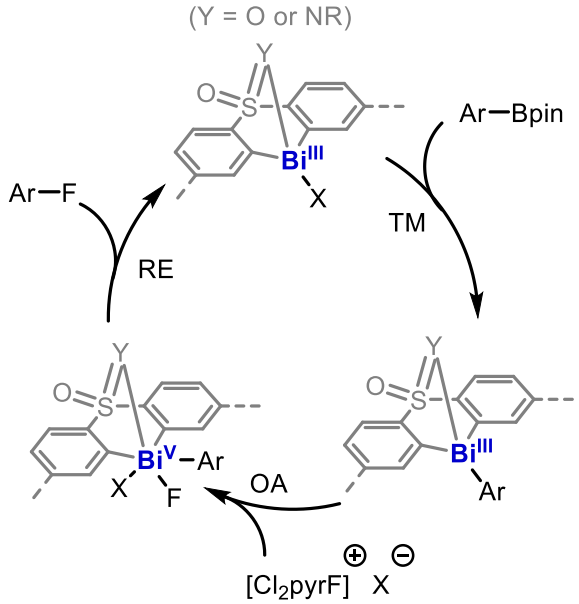

high-valent polar Bi-redox catalysis

For selected recent examples of low-valent polar Bi-redox catalysis, see: a) J. Cornella et al. *J. Am. Chem. Soc.* **2019**, *141*, 4235–4240;
b) J. Cornella et al. *J. Am. Chem. Soc.* **2020**, *142*, 19473–19479; c) J. Cornella et al. *J. Am. Chem. Soc.* **2021**, *143*, 12487–12493.
For selected recent examples of high-valent polar Bi-redox catalysis, see: a) J. Cornella et al. *Science* **2020**, *367*, 313–317;
b) L. T. Ball et al. *Nat. Chem.* **2020**, *12*, 260–269;c) J. Cornella et al. J. Am. Chem. Soc. 2022, 144, 14489–14504; d) L. T. Ball et al. *Angew. Chem. Int. Ed.* **2022**, *61*, e202210840.

1. 前言

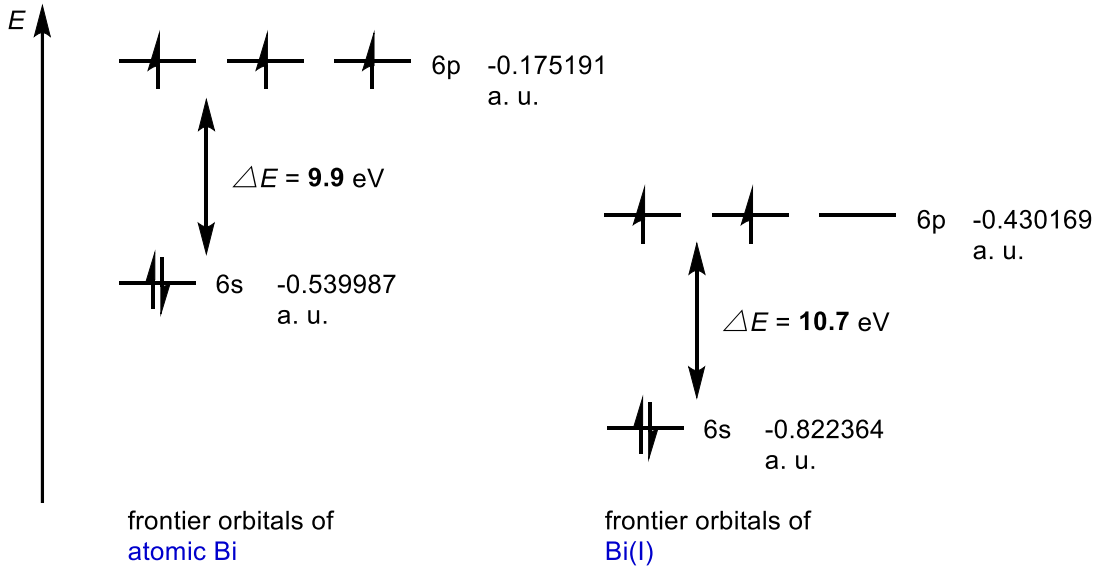

6s & 6p orbitals of bismuth are **large**, **diffuse** & **non-hybridized**

⇨ **weaker** Bi-E σ bonding: (Pn = P, As, Sb, Bi)

	PH_3	AsH_3	SbH_3	BiH_3	
Pn-H dissociation △*H* (kcal/mol)	81.4	74.6	63.3	51.8	smaller △*H*, weaker Pn-H bond

a) https://www.nist.gov/pml/atomic-reference-data-electronic-structure-calculations/atomic-reference-data-electronic-7-67 (data from ScRLDA approximation);
b) D. Dai, K. Balasubramanian, *J. Chem. Phys.* **1990**, *93*, 1837–1846;
c) K. Balasubramanian et al. *J. Chem. Phys.* **1993**, *98*, 8859–8869.

1. 前言

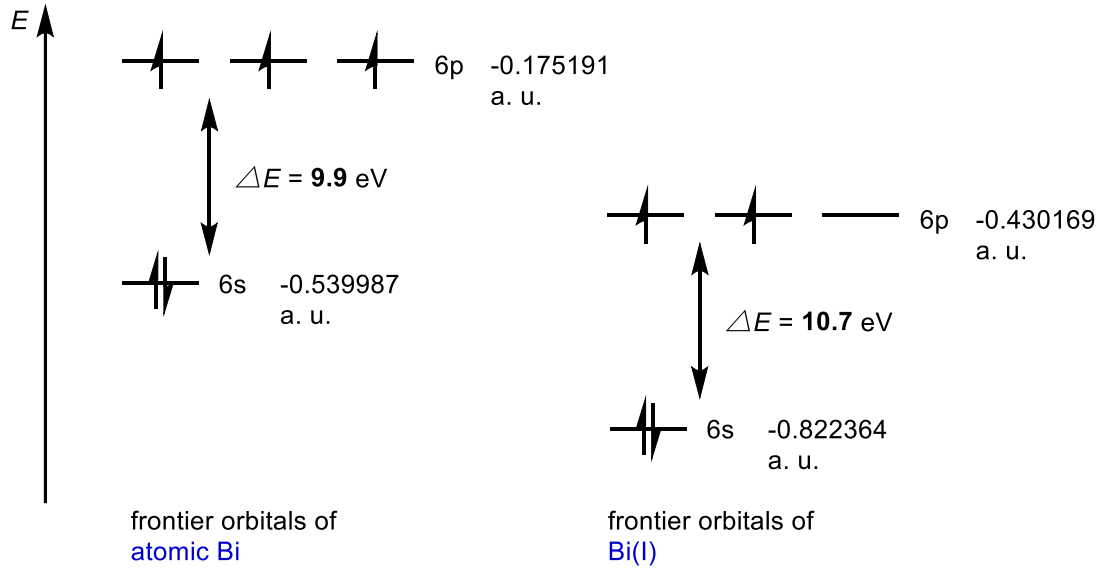

6s & 6p orbitals of bismuth are **large**, **diffuse** & **non-hybridized**

⇨ **weaker** Bi-E σ bonding: (Pn = P, As, Sb, Bi)

Pn-H dissociation △*H* (kcal/mol)	PH_3	AsH_3	SbH_3	BiH_3
	81.4	74.6	63.3	51.8

smaller △*H*, weaker Pn-H bond

Weak Bi-E σ bonding ⇨ **Facile** Bi(III)-E homolytic cleavage

Low Bi-E dissociation △*H* ⇨ Generation of **Bi(II)** radicals

2 selected hints of **Bi(II)** radical formation:

G. H. Williams (1963) & O. N. Druzhkov (1965):

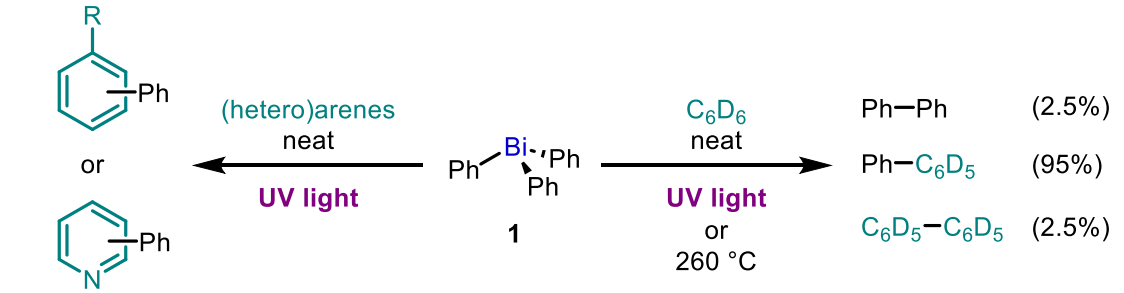

A. G. Davies (1971):

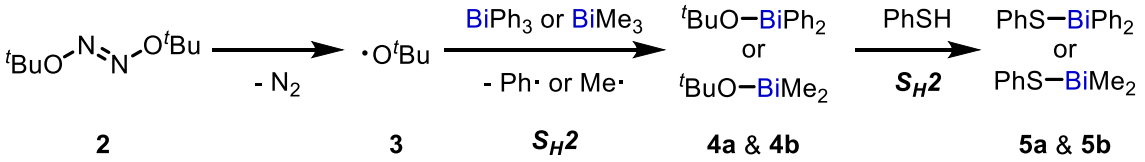

a) D. H. Hey, D. A. Shingleton, G. H. Williams, *J. Chem. Soc.* **1963**, 5612–5619;
b) G. A. Razuvaev, G. G. Petukhov, V. A. Titov, O. N. Druzhkov, *Zh. Org. Khim.* **1965**, *35*, 481–485;
c) A. G. Davies, S. C. W. Hook, *J. Chem. Soc. B* **1970**, 735–737; A. G. Davies, S. C. W. Hook, *J. Chem. Soc. C* **1971**, 1660–1665.

目录

2.1. 通过铋(III)单电子还原产生铋(II)中心自由基

T. Iwamoto (2014): first generation of a persistent **Bi(II)** radical

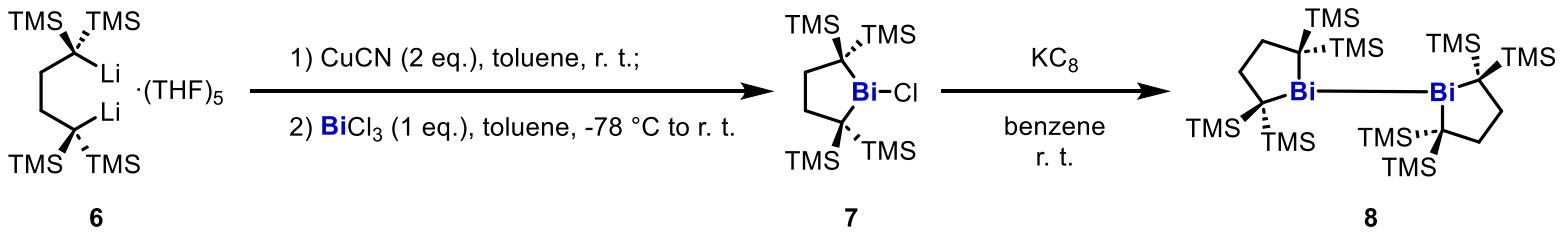

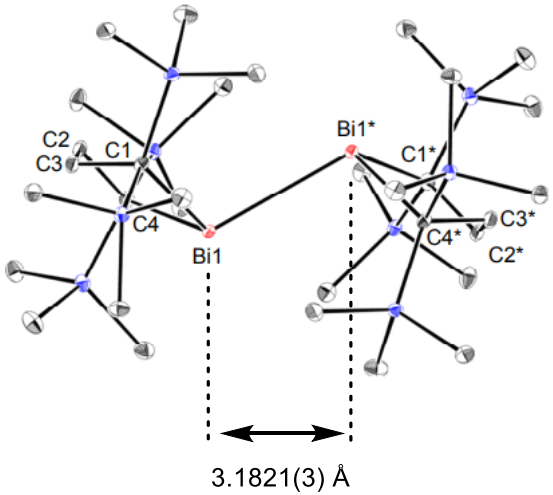

crystalline structure of **8**:
exceptionally long **Bi-Bi** distance

(previously reported distances:
2.9902(5) - 3.087(3) Å)

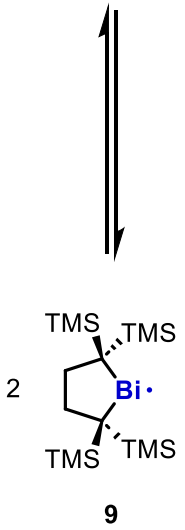

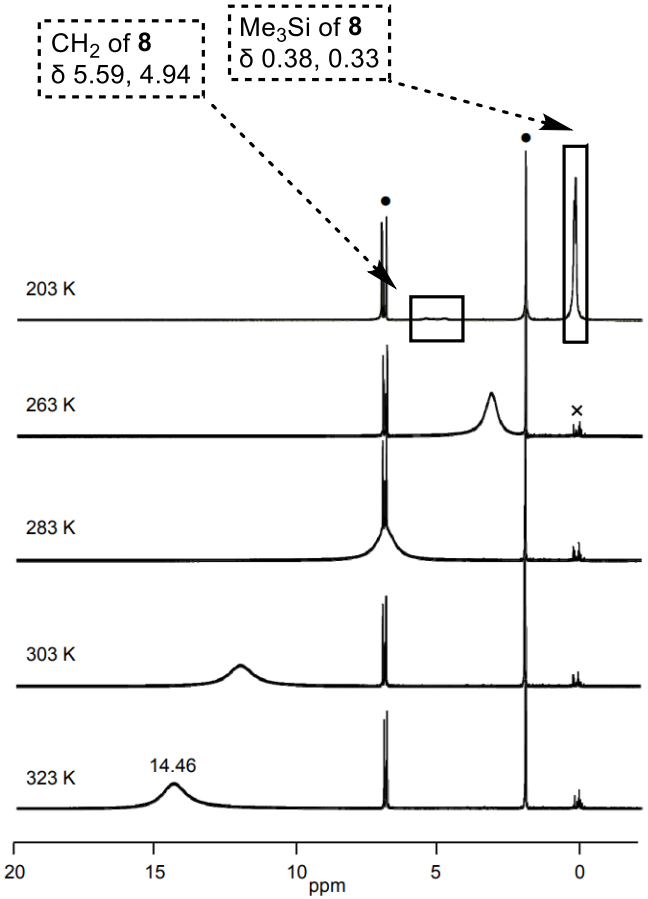

^{1}H NMR signals of dimer **8** vanish in d_7-toluene & a broad downfield signal appears as *T* rises.

T. Iwamoto et al. *Angew. Chem. Int. Ed.* **2014**, *53*, 11172–11176.

2.1. 通过铋(III)单电子还原产生铋(II)中心自由基

T. Iwamoto (2014): first generation of a persistent **Bi(II)** radical

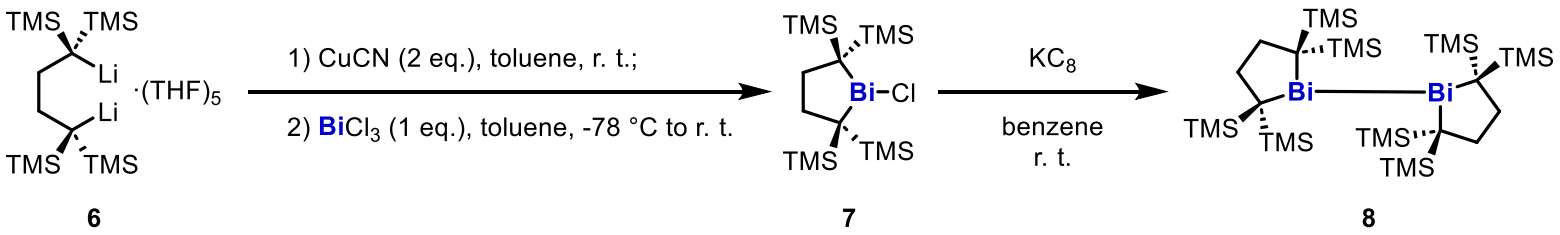

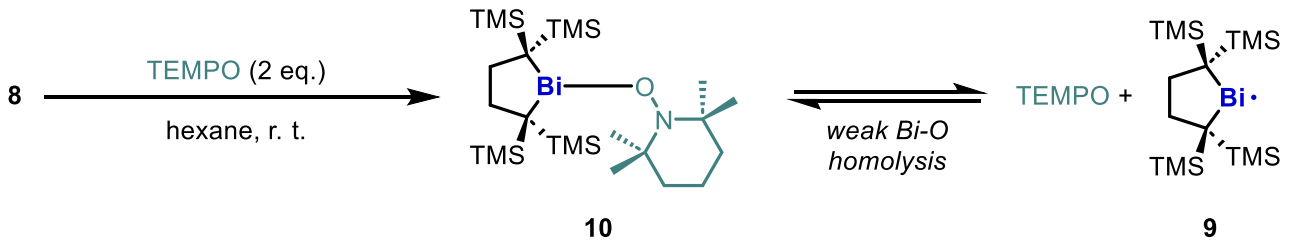

***Bi*-centered radical reactivity**
reversible bonding of Bi-O

T. Iwamoto et al. *Angew. Chem. Int. Ed.* **2014**, *53*, 11172–11176.

2.1. 通过铋(III)单电子还原产生铋(II)中心自由基

M. P. Coles (2015): first monomeric **Bi(II)** radical stable in the solid state

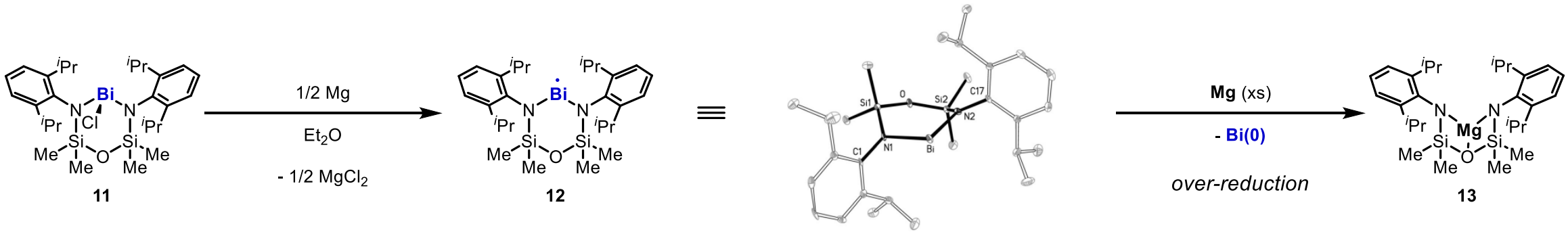

Stephen Schultz (2018):

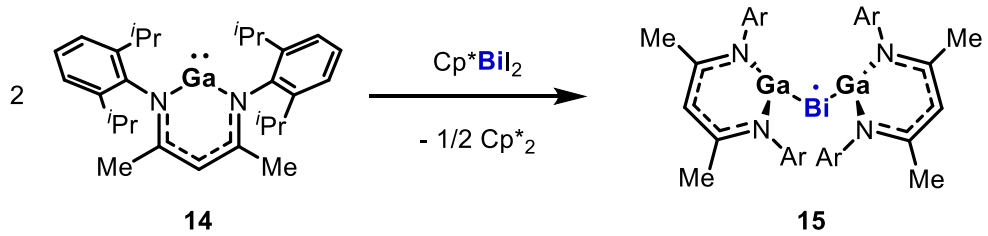

(Ar = 2,6-^{i}Pr$_2$-C$_6$H$_3$)

unpaired electron of **Bi(II)**
largely delocalized by **Ga(III)** centers

Axel Schultz (2018): **Bi(II) biradical**

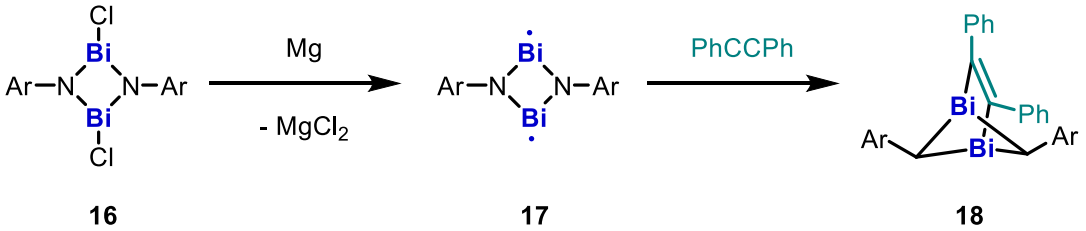

(Ar = 2,6-bis(2,4,6,-trimethylphenyl)-phenyl)

a) M. P. Coles et al. *Angew. Chem. Int. Ed.* **2015**, *54*, 10630–10633;
b) S. Schultz et al. *Nat. Commun.* **2018**, *9*, 87;
c) A. Schultz et al. *Dalton Trans.* **2018**, *47*, 4433–4436.

2.1. 通过铋(III)单电子还原产生铋(II)中心自由基

Z. R. Turner (2019): *N*,*N*,*N*-ligated **Bi(II)** radical generated by organic reductant & subsequent C(sp^3)-O bond activation

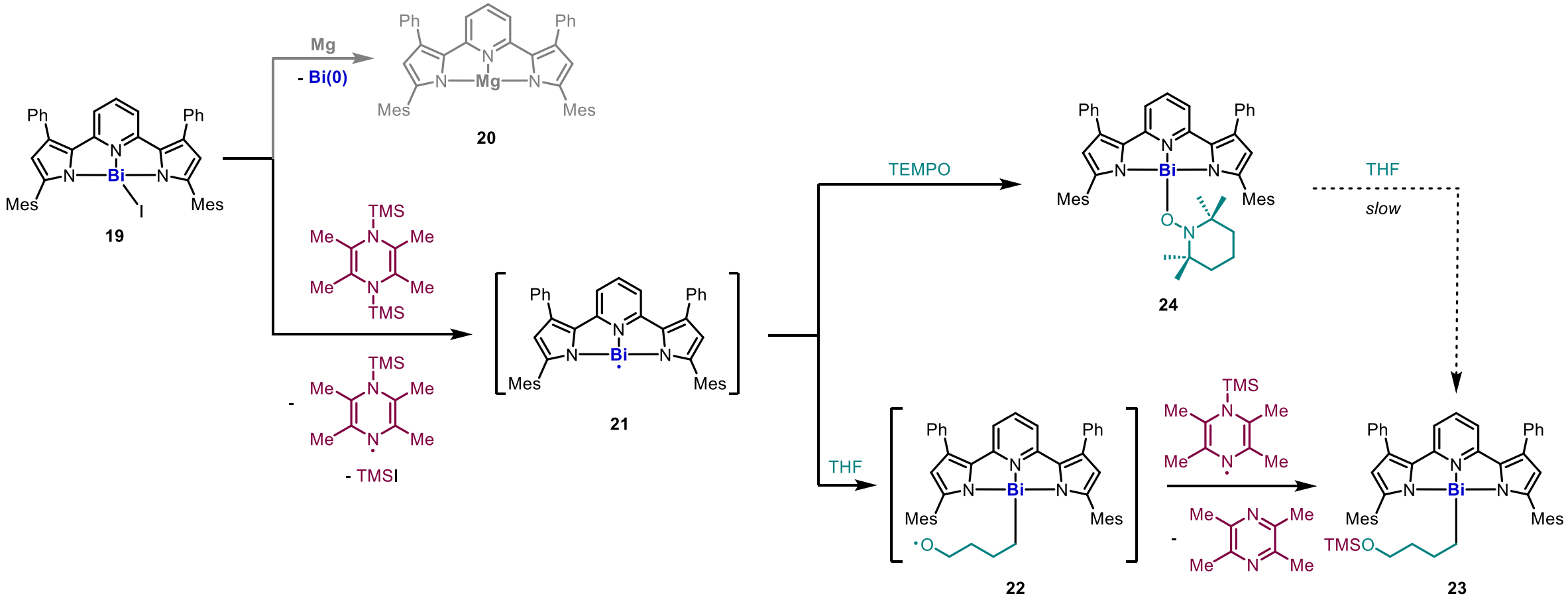

Z. R. Turner, *Inorg. Chem.* **2019**, *58*, 14212–14227.

2.1. 通过铋(III)单电子还原产生铋(II)中心自由基

J. Abbenseth (2025): first crystalline **Bi(II)** radical anion

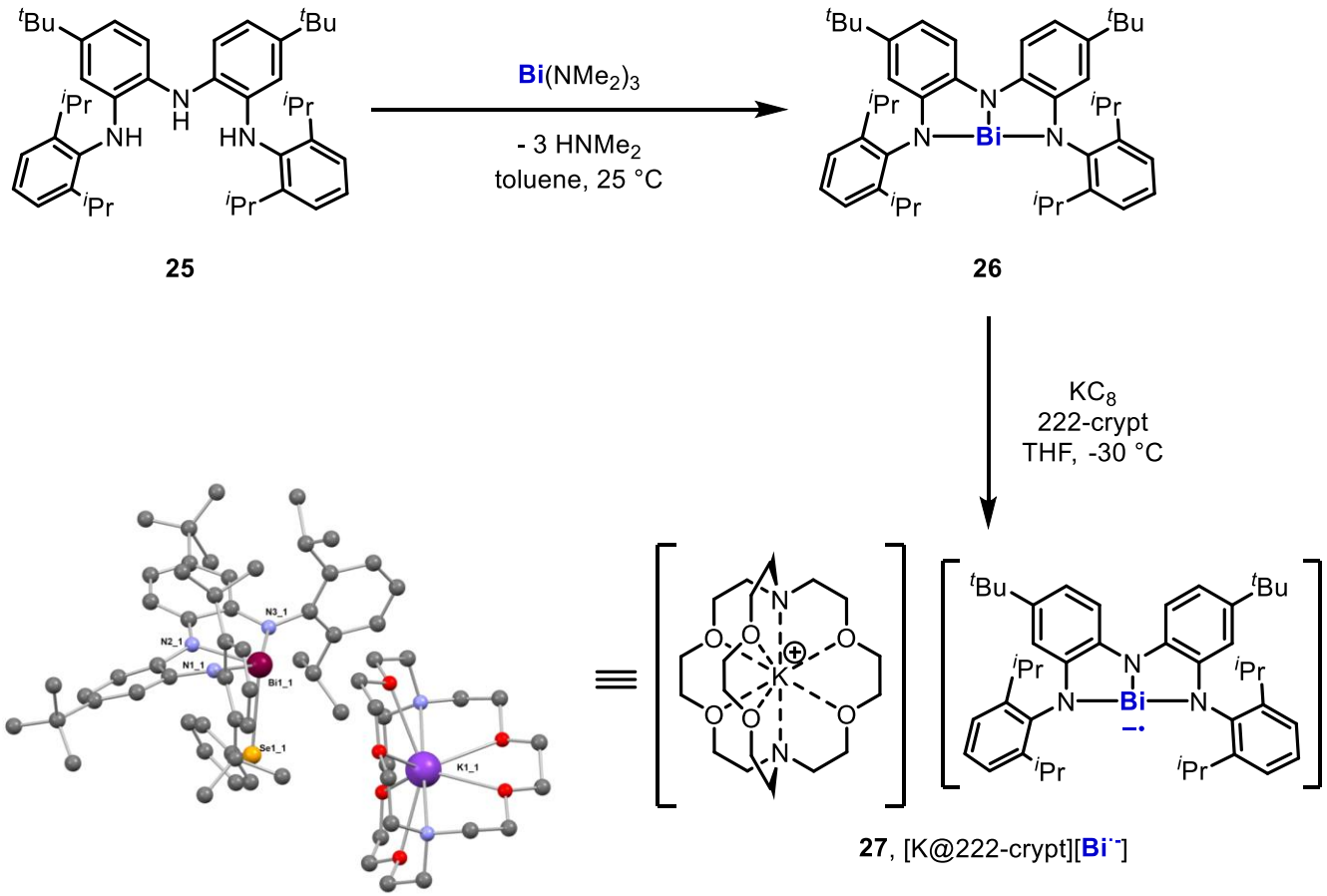

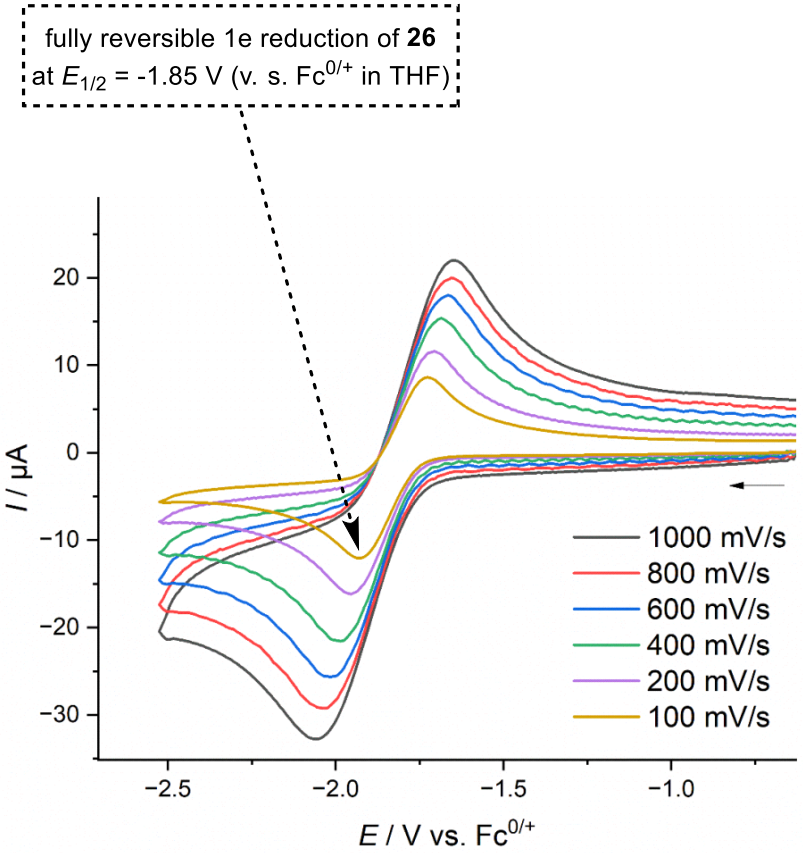

J. Abbenseth et al. *Angew. Chem. Int. Ed.* **2025**, e202515545.

2.1. 通过铋(III)单电子还原产生铋(II)中心自由基

J. Abbenseth (2025): first crystalline **Bi(II)** radical anion

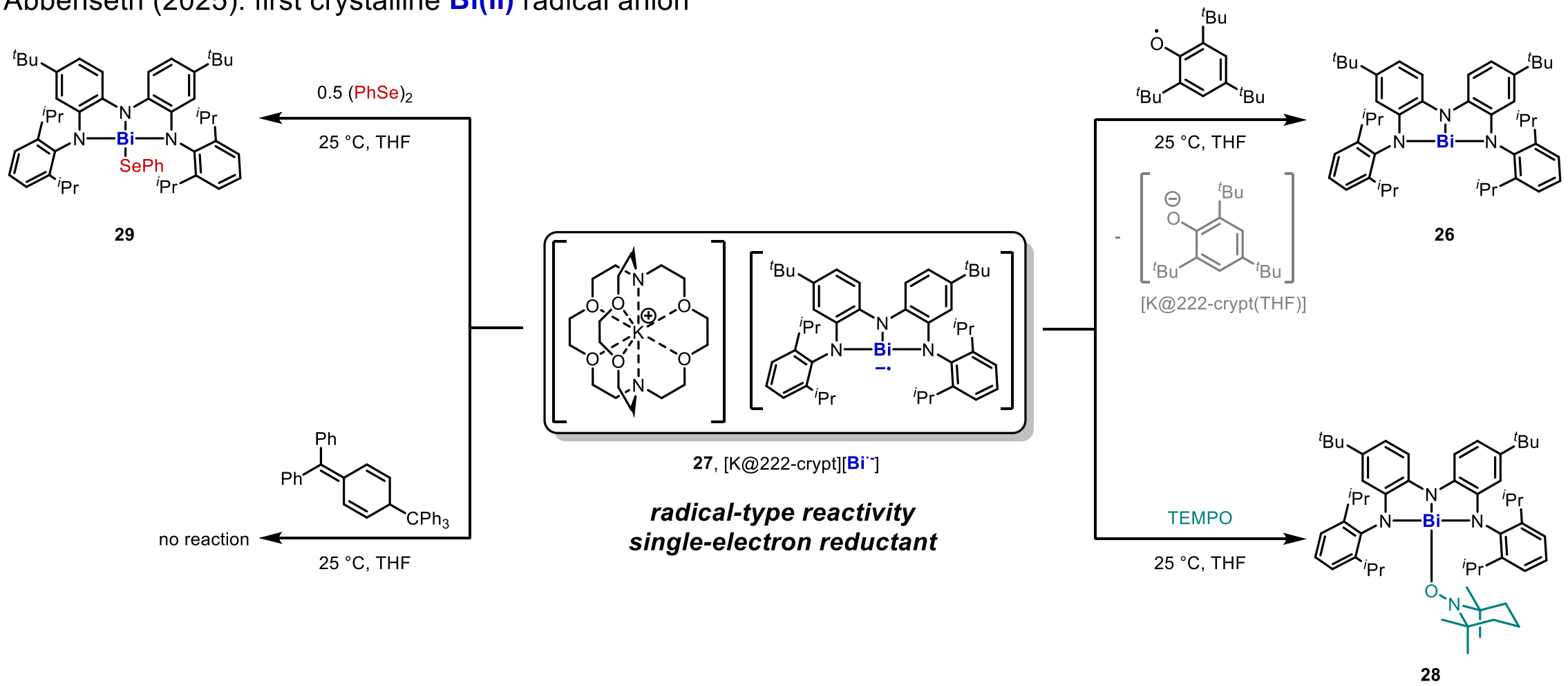

J. Abbenseth et al. *Angew. Chem. Int. Ed.* **2025**, e202515545.

2.2. 通过铋(I)单电子氧化产生铋(II)中心自由基

J. D. Corbett (1958): solid state synthesis of **Bi(I)**

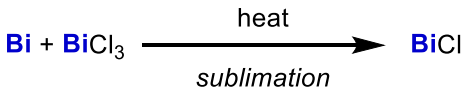

L. Andrews (2003): laser-ablated generation of **Bi(I)**

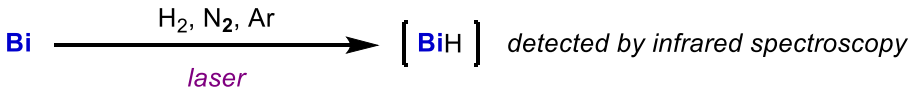

L. Dostál (2010): first synthesis of monomeric *N*,*C*,*N*-stablized singlet **Bi(I)** compund

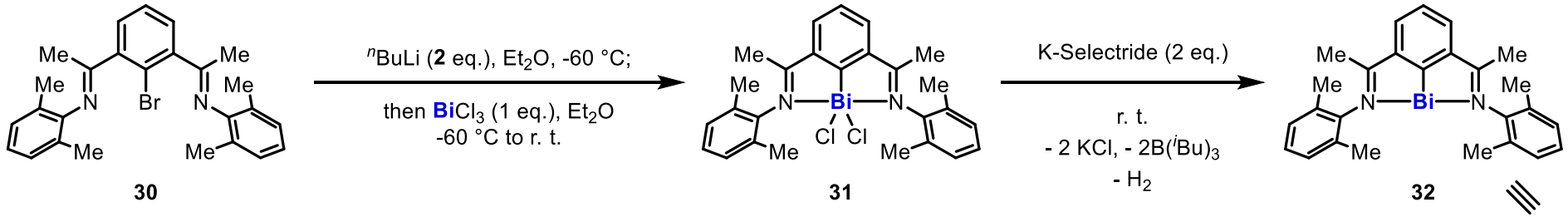

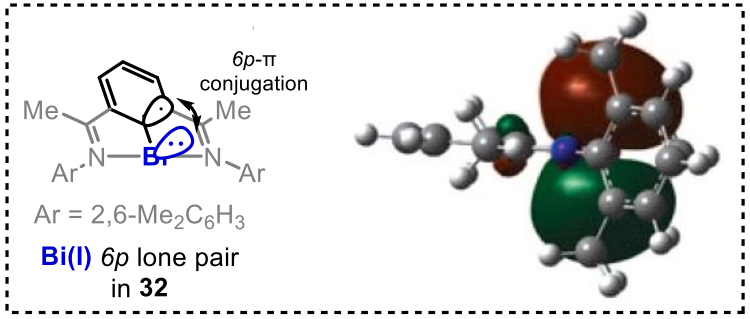

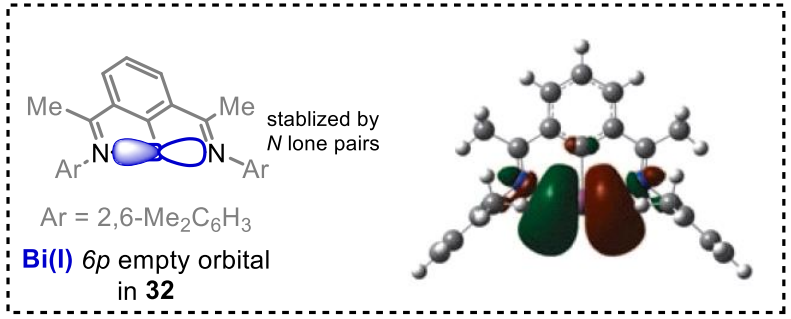

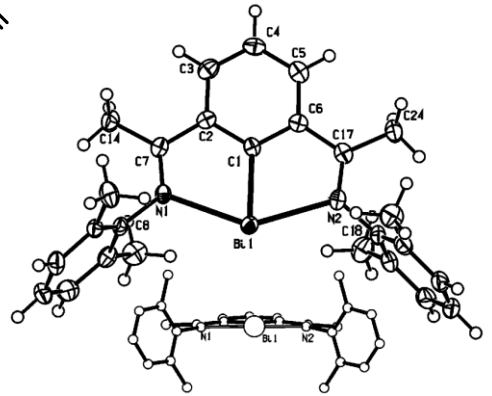

a) J. D. Corbett, *J. Am. Chem. Soc.* **1958**, *80*, 4757–4760; J. D. Corbett, *J. Phys. Chem.* **1958**, *62*, 1149–1150;
b) X. Wang, P. F. Souter, L. Andrews, *J. Phys. Chem. A* **2003**, *107*, 4244–4249;
c) L. Dostál et al. *Angew. Chem. Int. Ed.* **2010**, *49,* 5468–5471.

2.2. 通过铋(I)单电子氧化产生铋(II)中心自由基

L. Dostál (2010): first synthesis of monomeric *N*,*C*,*N*-stablized singlet **Bi(I)** compund

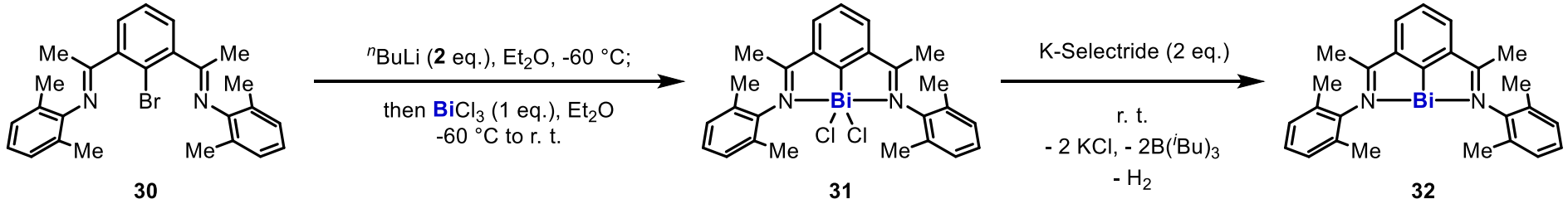

Josep Cornella (2021 & 2023):

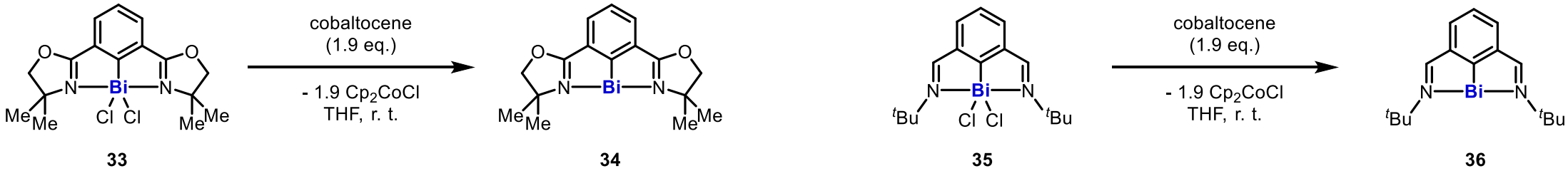

a) L. Dostál et al. *Angew. Chem. Int. Ed.* **2010**, *49,* 5468–5471.
b) J. Cornella et al. *J. Am. Chem. Soc.* **2021**, *143*, 12487–12493; J. Cornella et al. *Angew. Chem. Int. Ed.* **2023**, *62*, e202313578.

2.2. 通过铋(I)单电子氧化产生铋(II)中心自由基

Josep Cornella (2023): first synthesis of two **Bi(II)** radical cation complexes

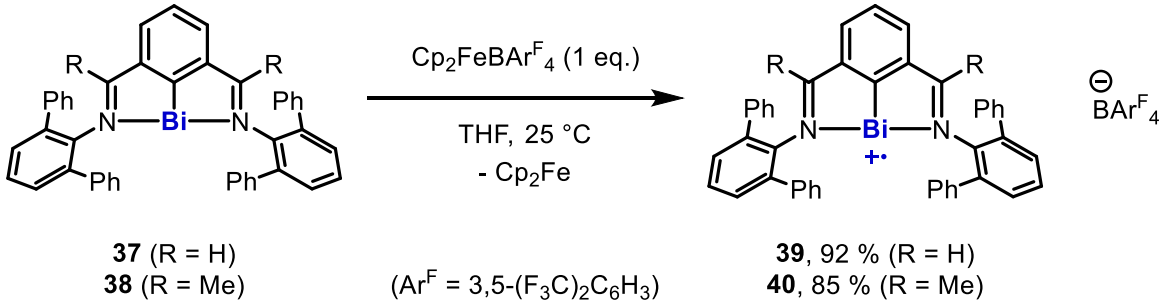

37 (R = H)
38 (R = Me)

(Ar^F = 3,5-$(F_3C)_2C_6H_3$)

39, 92 % (R = H)
40, 85 % (R = Me)

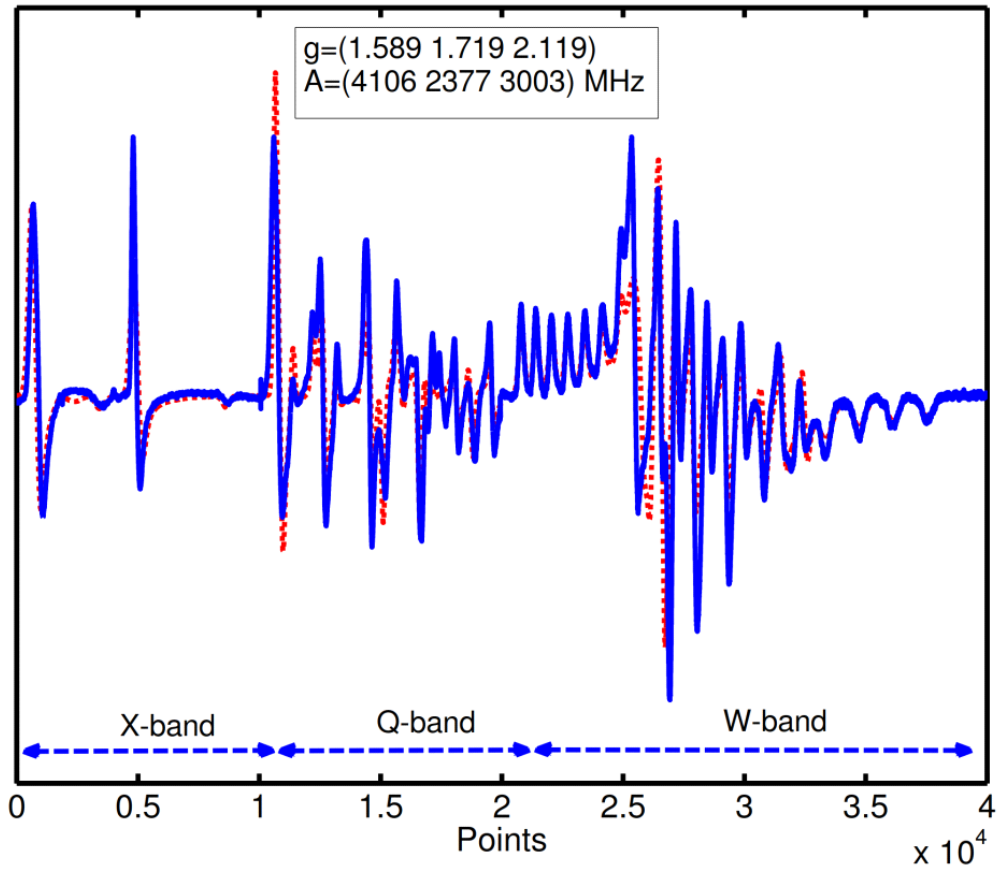

EPR spectra (blue) & simulation (red) of compound **40** showing *S* = 1/2

J. Cornella et al. *J. Am. Chem. Soc.* **2023**, *145*, 5618–5623.

2.3. 通过铋(III)-杂原子键均裂产生铋(II)中心自由基

R. J. Errington & N. C. Norman (1991):

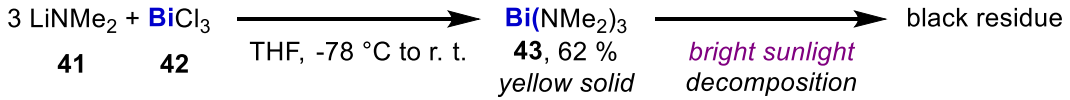

J. Lorberth (1995): light-sensitivity of **Bi**Cp_3

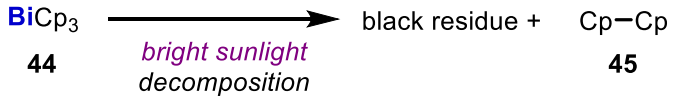

T. A. Hanna (2002 & 2009): **Bi(III)**-O homolysis of bismuth phenolates

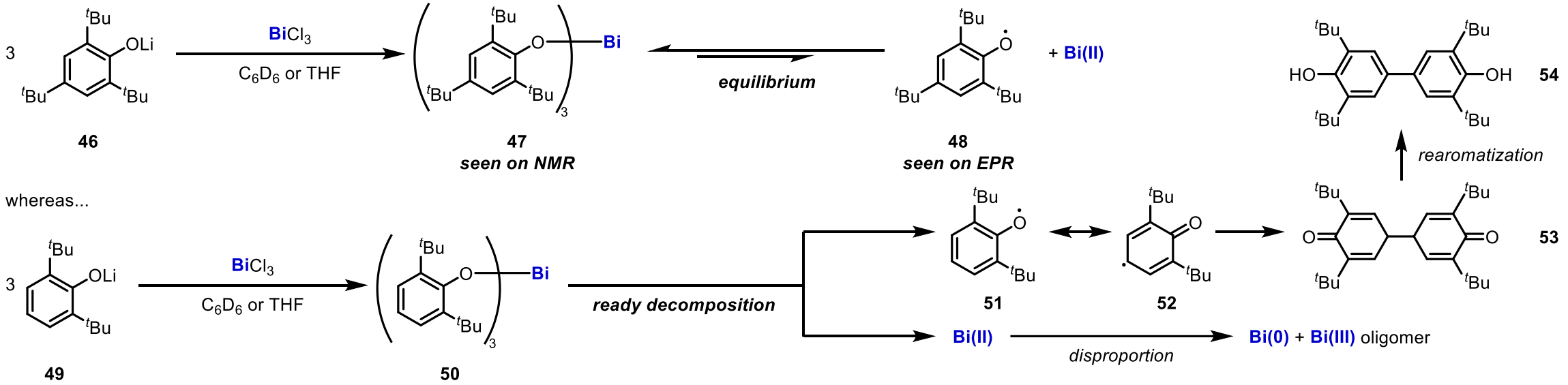

a) R. J. Errington, N. C. Norman et al. *Inorg. Chem.* **1991**, *30*, 4680–4682; J. Lorberth et al. *J. Organomet. Chem.* **1995**, *485*, 149–152;
b) T. A. Hanna et al. *Inorg, Chem.* **2002**, *41*, 3590–3592; T. A. Hanna et al. *Inorg. Chem.* **2009**, *48*, 11002–11016.

2.3. 通过铋(III)-杂原子键均裂产生铋(II)中心自由基

Axel Schultz (2016): homolysis of **Bi(III)**-N bond

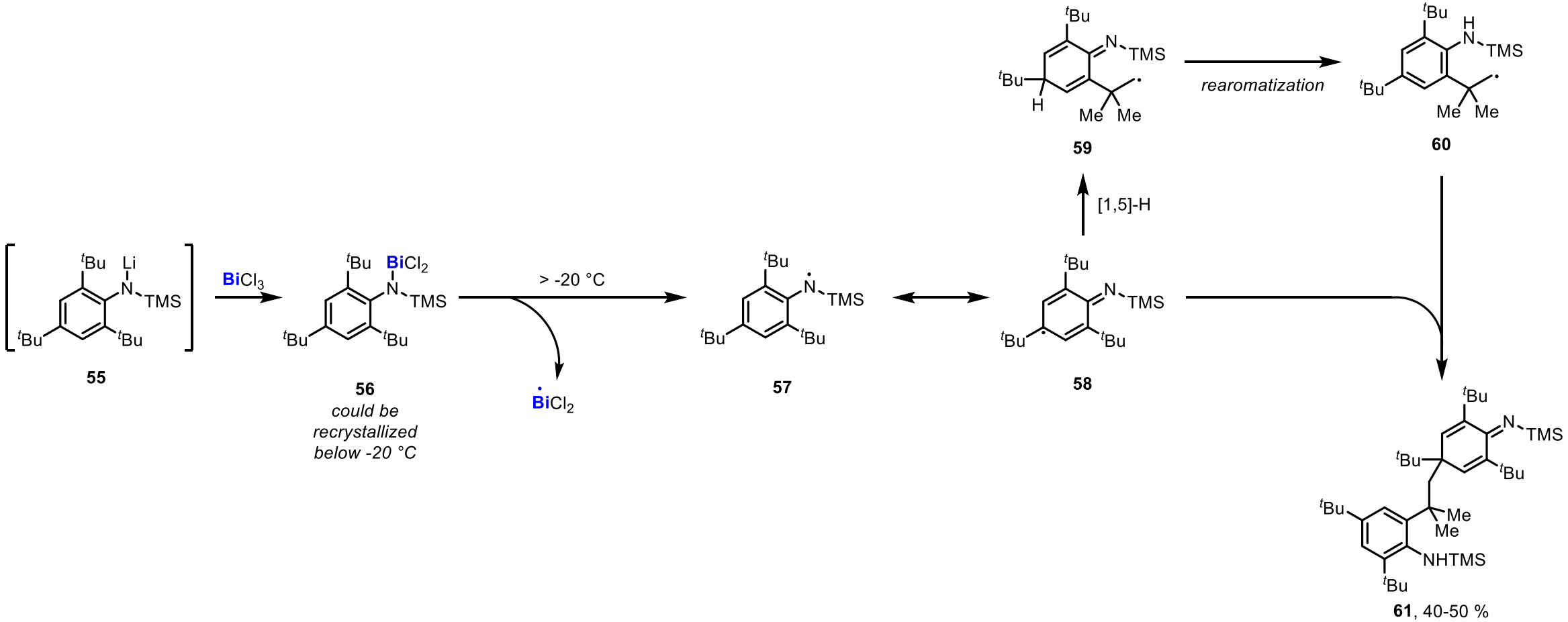

A. Schultz et al. *Dalton Trans.* **2016**, *45*, 6053–6059.

2.3. 通过铋(III)-杂原子键均裂产生铋(II)中心自由基

W. J. Evans (2011): unprecedented formation of a monodentate carbon-bound oxyaryl dianion

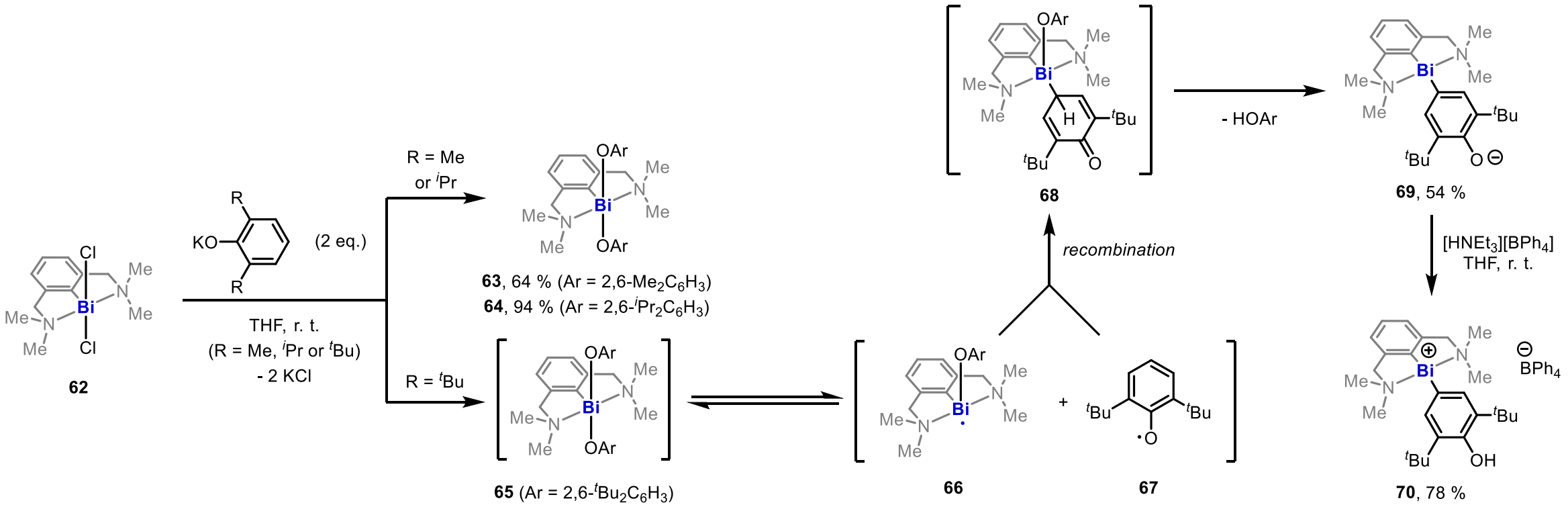

W. J. Evans et al. *J. Am. Chem. Soc.* **2011**, *133*, 5244–5247.

2.3. 通过铋(III)-杂原子键均裂产生铋(II)中心自由基

Josep Cornella (2022): radical activation of strong N-H and O-H bonds *via* **Bi(III)**-O homolytic cleavage

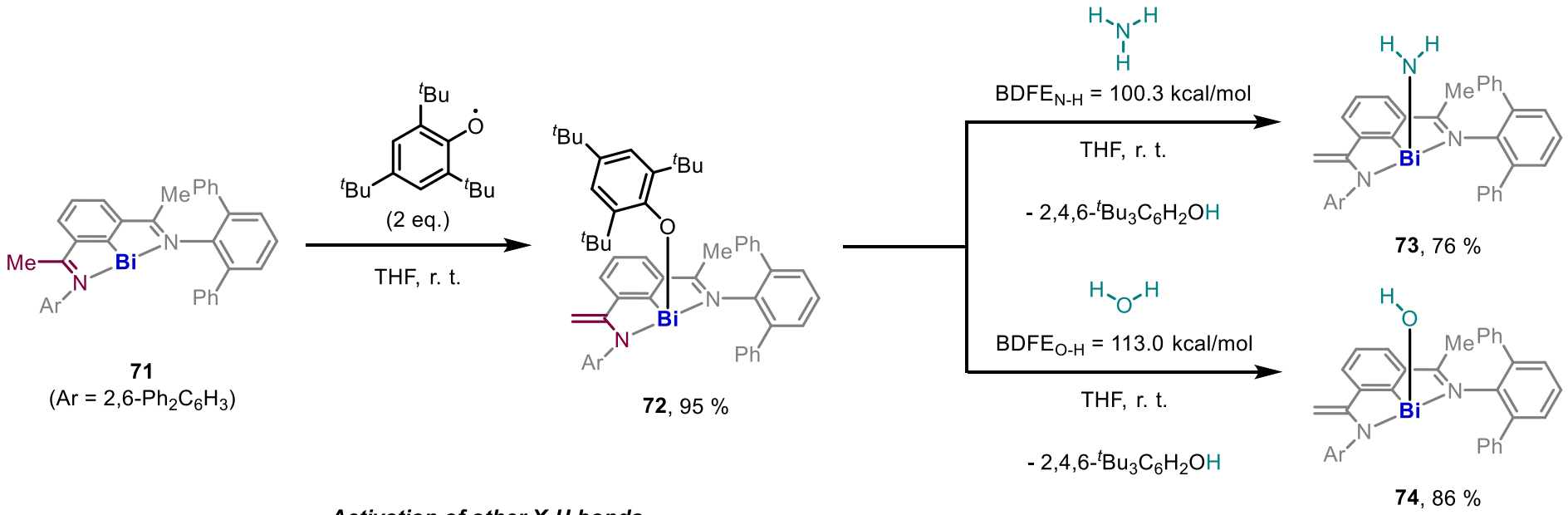

Activation of other X-H bonds

BDFE (kcal/mol)	79.8	97.0	90.7	95.0
yield of resultant **Bi** complex	92 %	98 %	95 %	78 %

J. Cornella et al. *J. Am. Chem. Soc.* **2022**, *144*, 16535–16544.

2.4. 三线态铋宾的合成与性质

C. Lichtenberg (2020): generation & analysis of the first diradical-type bismuthinidene

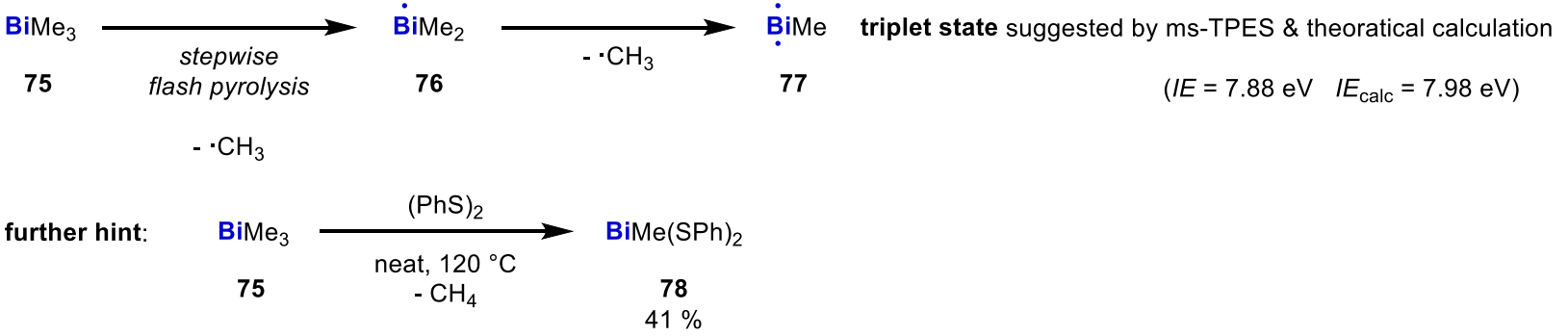

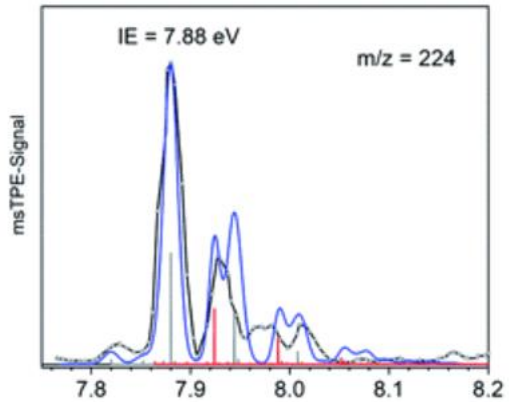

N. Tokitoh (1997) & P. P. Power (1999): yield of dibismuthene *via* reduction of **Bi(III)** compounds

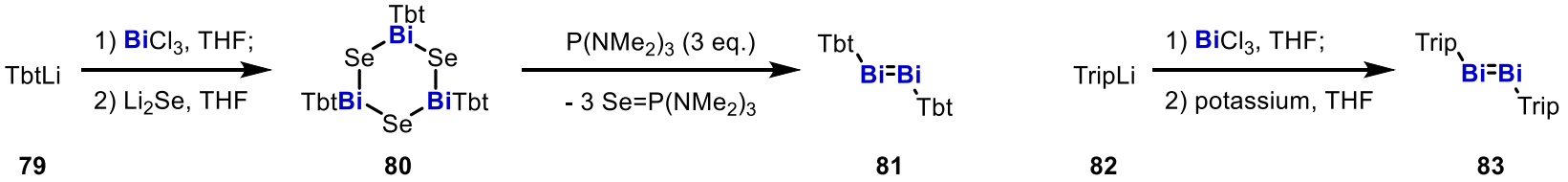

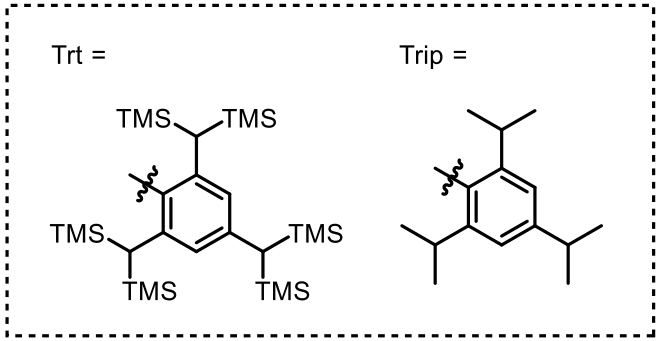

a) C. Lichtenberg et al. *Chem. Sci.* **2020**, *11*, 7562–7568;
b) N. Tokitoh et al. *Science* **1997**, *277*, 78–80; P. P. Power et al. *J. Am. Chem. Soc.* **1999**, *121*, 3357–3367.

2.4. 三线态铋宾的合成与性质

Frank Neese & Josep Cornella (2023): first synthesis & isolation of a hindered triplet bismuthinidene

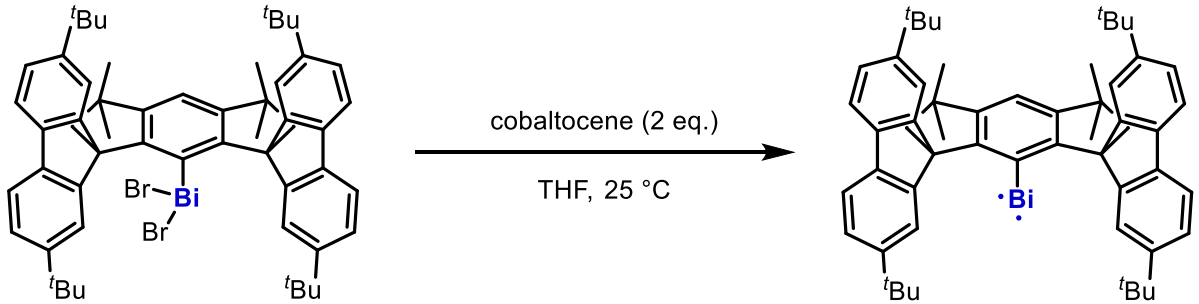

84 **85**
81 %

reactivity of **85**

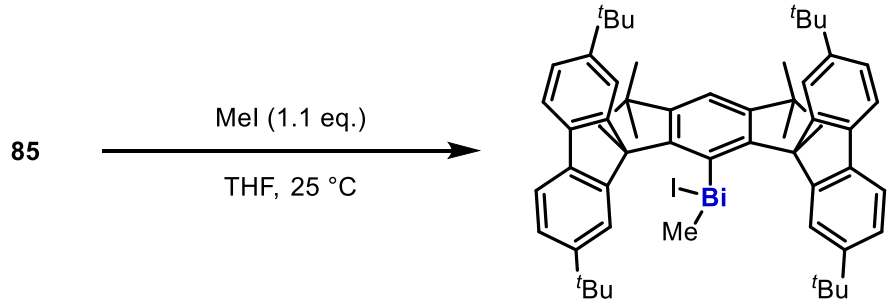

86
84 %

NMR behavior of **85**

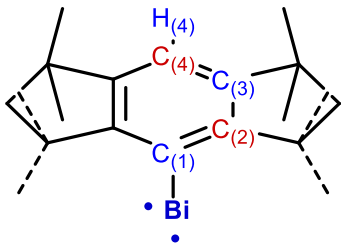

atoms		δ (ppm)
$C_{(1)}$	shielded	-203.8
$C_{(2)}$	deshielded	234.0
$C_{(3)}$	shielded	114.5
$C_{(4)}$	deshielded	160.0
$H_{(4)}$	shielded	-1.06

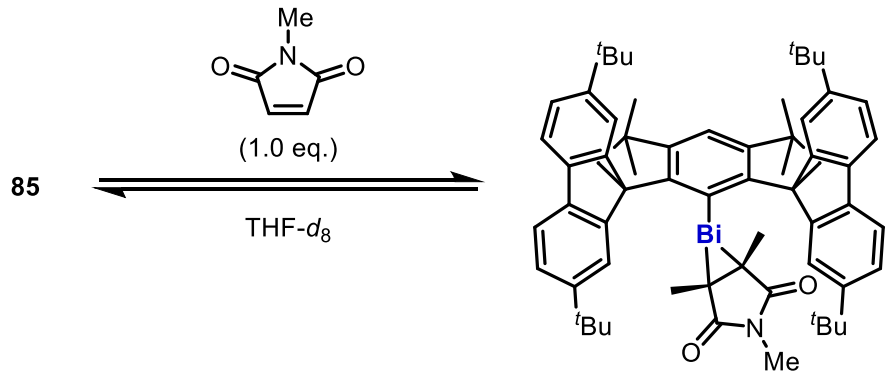

87

F. Neese, J. Cornella et al. *Science* **2023**, *380*, 1043– 1048.

目录

3.1. 铋催化的自由基型聚合反应

S. Yamago (2007): **Bi**-catalyzed living radical polymerization

(*first synthetic example where catalytic bismuth are involved in radical processes*)

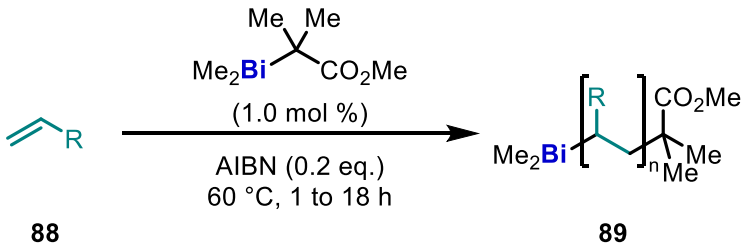

Scope of olefin monomers

	Ph	$CO_2{}^nBu$	$CONH^iPr$	N-vinylpyrrolidone
Conversion (%)	100	97	94	94
M_n	10500	11000	12200	11100
PDI	1.09	1.10	1.10	1.06

mechanism of polymerization

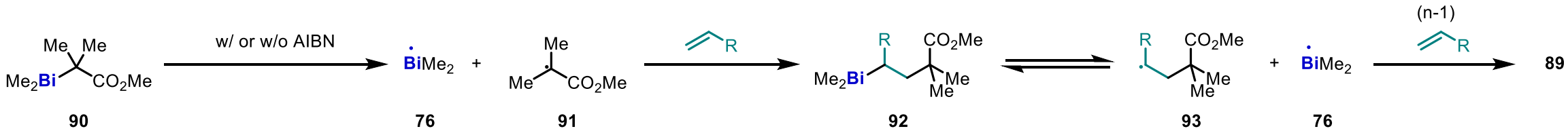

S. Yamago et al. *Angew. Chem. Int. Ed.* **2007**, *46*, 1304–1306.

3.1. 铋催化的自由基型聚合反应

S. Yamago (2007): **Bi**-catalyzed living radical polymerization (**BIRP**)

(*first synthetic example where catalytic bismuth are involved in radical processes*)

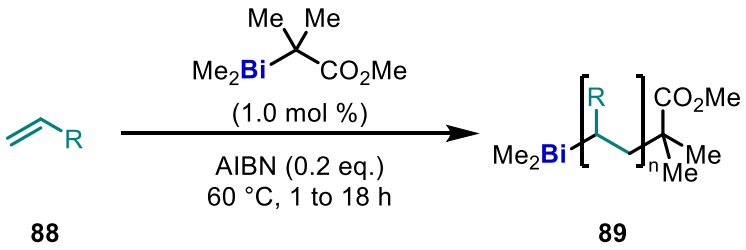

88 **89**

Scope of olefin monomers

	Ph	$CO_2{}^nBu$	$CONH^iPr$	N-vinylpyrrolidone
Conversion (%)	100	97	94	94
M_n	10500	11000	12200	11100
PDI	1.09	1.10	1.10	1.06

effective catalysts for **BIRP**

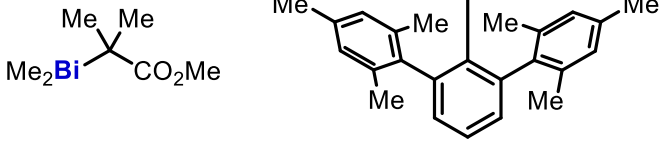

90
Yamago (2007)

94
Yamago (2009)

Bi(allyl)$_3$

95
Lichtenberg (2012)

$\oplus$ **Bi**(allyl)$_2$(THF)$_2$

96
Lichtenberg (2012)

a) S. Yamago et al. *Angew. Chem. Int. Ed.* **2007**, *46*, 1304–1306;
b) S. Z. Zard et al. *Tetrahedron* **1989**, *45*, 2615–2626; E. Kayahara, S. Yamago, *J. Am. Chem. Soc.* **2009**, *131*, 2508– 2513;
c) C. Lichtenberg, *Angew. Chem. Int. Ed.* **2012**, *51*, 13011–13015.

3.2. 铋催化的自由基型环化反应

C. Lichtenberg (2019): **Bi**-Mn-catalyzed cycloisomerization of alkenyl iodides

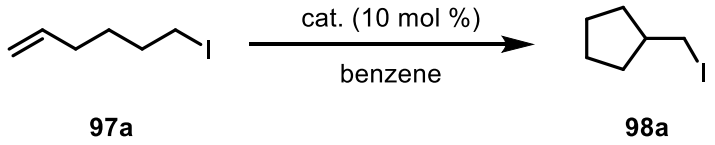

97a **98a**

catalyst	conditions	NMR yield
99	80 °C, 20 h	4
100	60 °C, 20 h	24
101	60 °C, 20 h	73
102	60 °C, 20 h, **light**	96
102	60 °C, 20 h, **dark**	95

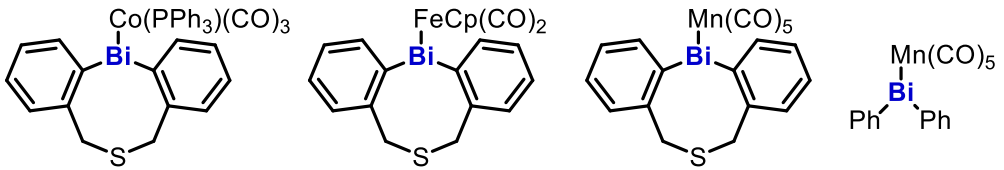

99 **100** **101** **102**

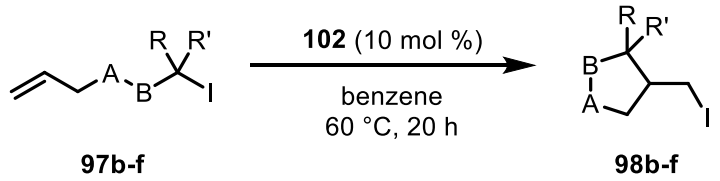

97b-f **98b-f**

Substrate scope[a]

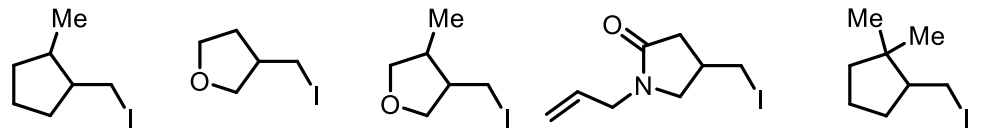

98b	**98c**[b]	**98d**	**98e**	**98f**[c]
> 99 %	83 %	> 99 %	> 95 %	90 %

[a] All yields were determined by ^{1}H-NMR or GC/MS analysis;
[b] 20 mol % **102**; [c] *T* = 23 °C.

radical trapping

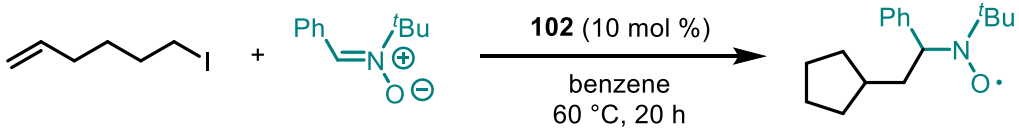

97a **103** **104**

EPR active

J. Ramler, I. Krummenacher, C. Lichtenberg, *Angew. Chem. Int. Ed.* **2019**, *58*, 12924–12929.

3.2. 铋催化的自由基型环化反应

C. Lichtenberg (2019): **Bi**-Mn-catalyzed cycloisomerization of alkenyl iodides

possible mechanism

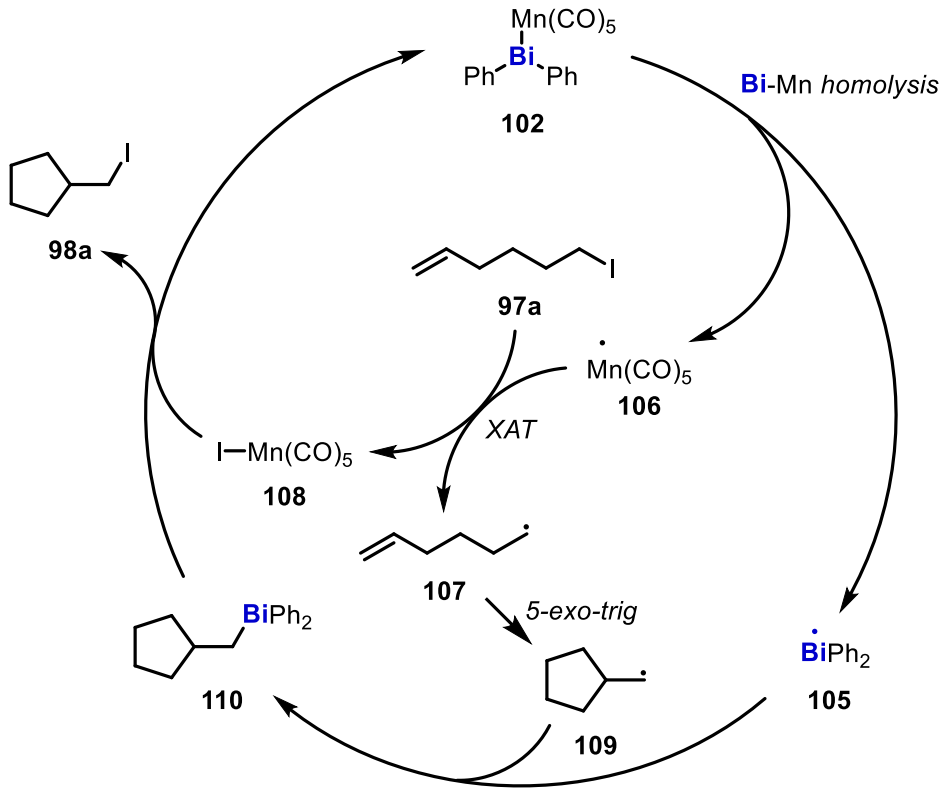

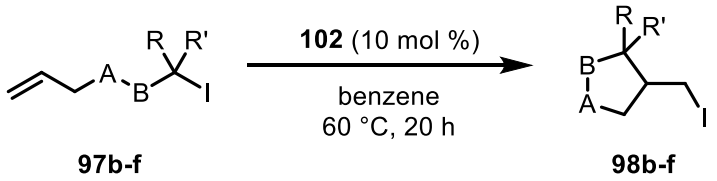

Substrate scope[a]

98b	98c[b]	98d	98e	98f[c]
> 99 %	83 %	> 99 %	> 95 %	90 %

[a] All yields were determined by ^{1}H-NMR or GC/MS analysis;
[b] 20 mol % **102**; [c] T = 23 °C.

radical trapping

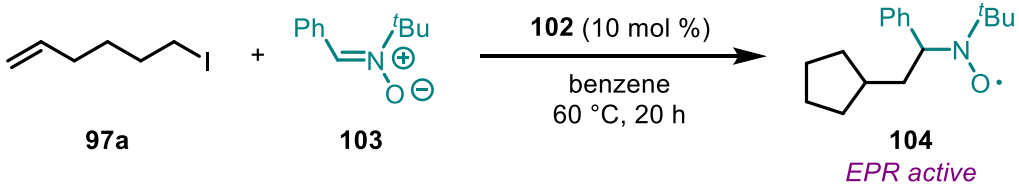

J. Ramler, I. Krummenacher, C. Lichtenberg, *Angew. Chem. Int. Ed.* **2019**, *58*, 12924–12929.

3.2. 铋催化的自由基型环化反应

Josep Cornella (2024): **Bi**-catalyzed reductive cyclopropanation

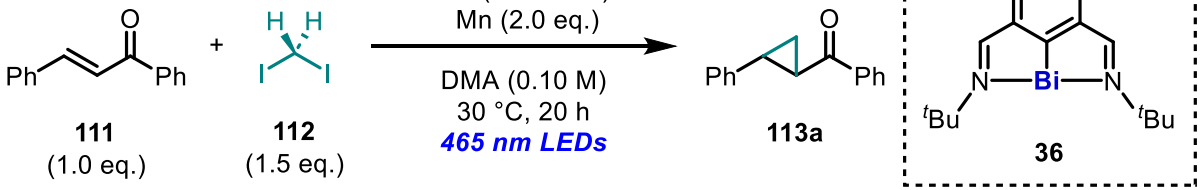

entry	deviations from above	NMR yield of **113a** (%)
1	none	74
2	w/o catalyst	trace
3	w/o light	trace
4	*red LEDs*	trace
5	MeCN instead of DMA	51
6	Zn instead of Mn	30
7	**35** instead of **36**	68
8	CH_2Br_2/NaI instead of CH_2I_2	40

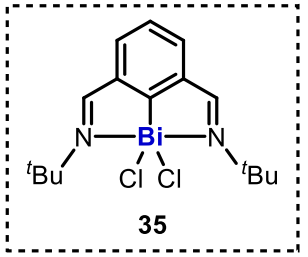

Scope of intermolecular cyclopropanation w/ enones[a][b][c]

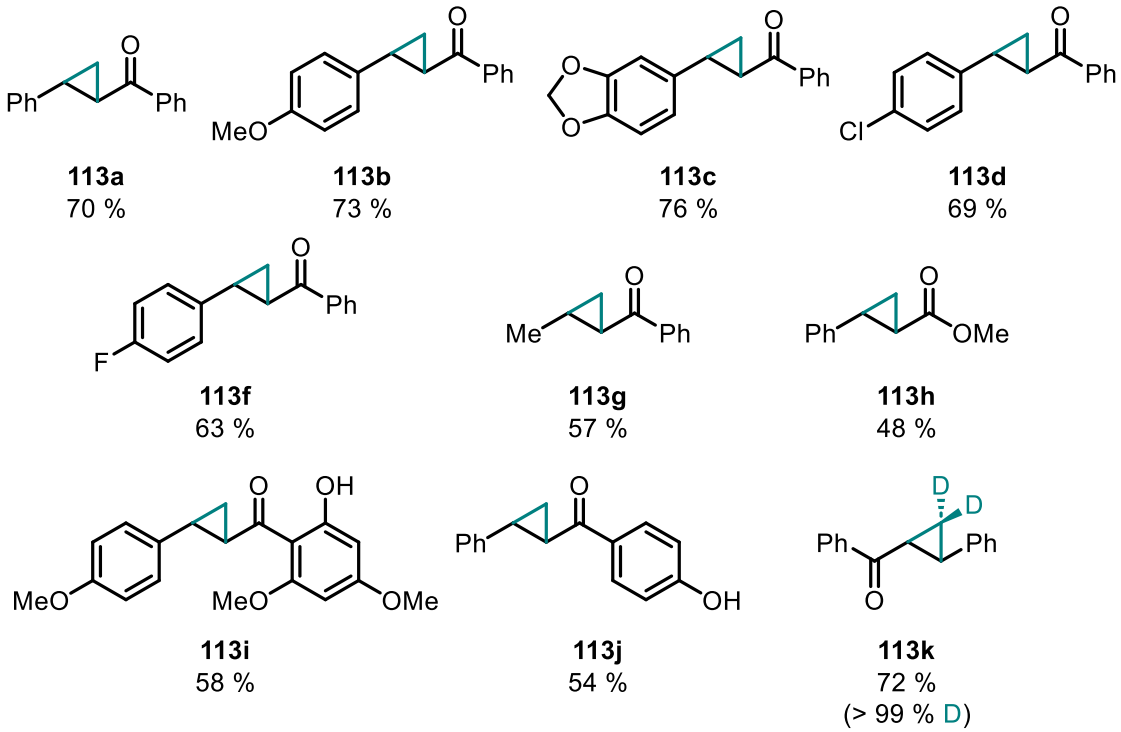

[a] Conditions: **36** (10 mol %), Mn (2.0 eq.), DMA (0.10 M), 30 °C, 24 h, 465 nm LEDs;
[b] Isolated yield;
[c] From *E*/*Z* alkene > 20:1; all the products possessing 2 stereocenters have a *trans* configuration; the substrates have a d. r. > 20:1 unless otherwise specified.

S. Ni, D. Spinnato, J. Cornella, *J. Am. Chem. Soc.* **2024**, *146*, 22140−22144.

3.2. 铋催化的自由基型环化反应

Josep Cornella (2024): **Bi**-catalyzed reductive cyclopropanation

Selected scope of intermolecular cyclopropanation w/ β-styrenes[a][b]

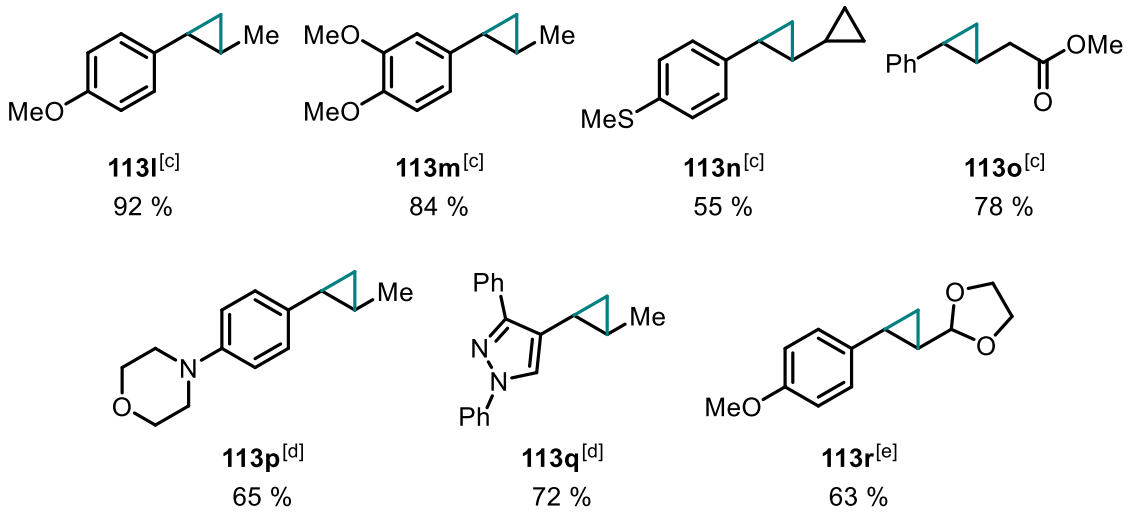

113l[c] 92 %　**113m**[c] 84 %　**113n**[c] 55 %　**113o**[c] 78 %

113p[d] 65 %　**113q**[d] 72 %　**113r**[e] 63 %

[a] Conditions: **35** (10 mol %), Mn (2.0 eq.), MeCN (0.10 M), 30 °C, 24 h, 465 nm LEDs;
[b] Isolated yield; all the products possessing 2 stereocenters have a *trans* configuration; the substrates have a d. r. > 20:1 unless otherwise specified;
[c] From *E*/*Z* alkene > 20:1; [d] From *E*/*Z* alkene = 1:4; [e] From *E*/*Z* alkene = 1.8:1.

Selected scope of inramolecular cyclopropanation[a][b]

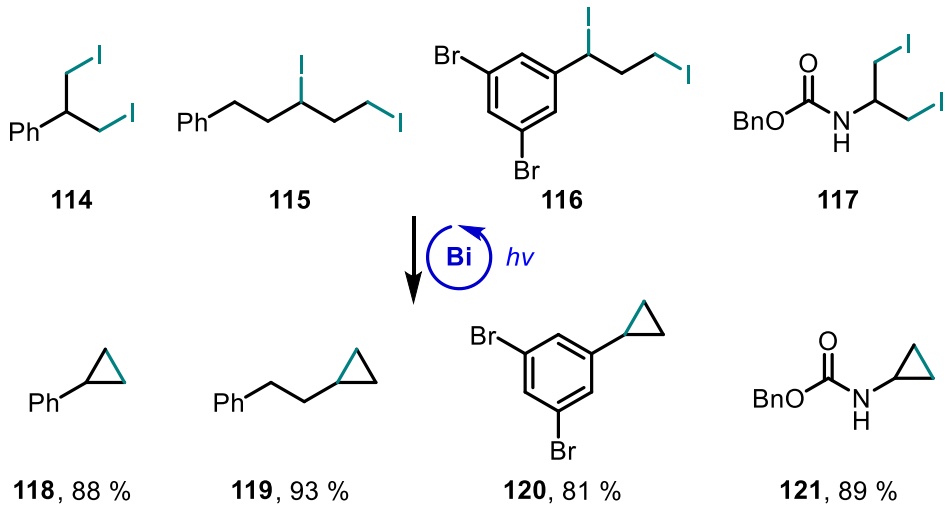

114　**115**　**116**　**117**

118, 88 %　**119**, 93 %　**120**, 81 %　**121**, 89 %

[a] Conditions: **35** (10 mol %), Mn (2.0 eq.), MeCN (0.10 M), 30 °C, 24 h, 465 nm LEDs;
[b] Isolated yield.

S. Ni, D. Spinnato, J. Cornella, *J. Am. Chem. Soc.* **2024**, *146*, 22140−22144.

3.2. 铋催化的自由基型环化反应

Josep Cornella (2024): **Bi**-catalyzed reductive cyclopropanation

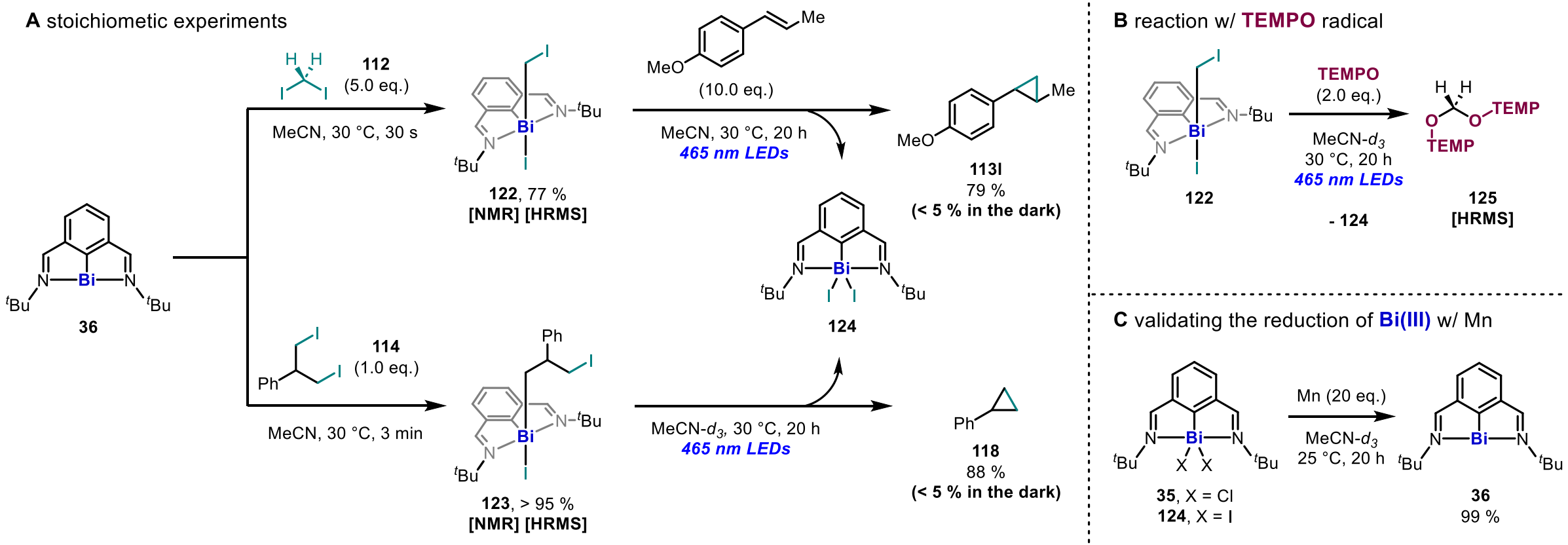

S. Ni, D. Spinnato, J. Cornella, *J. Am. Chem. Soc.* **2024**, *146*, 22140−22144.

3.2. 铋催化的自由基型环化反应

Josep Cornella (2024): **Bi**-catalyzed reductive cyclopropanation

D possible mechamism: **Bi(I/III/II/III)** catalytic cycle

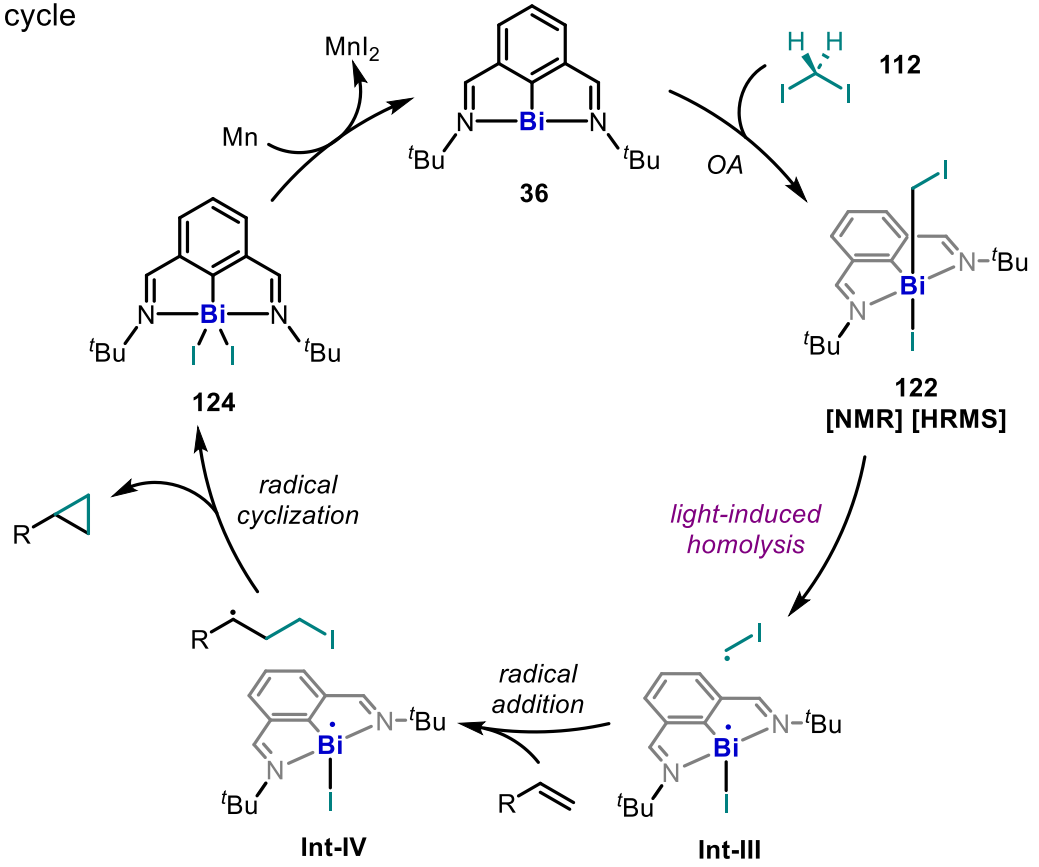

S. Ni, D. Spinnato, J. Cornella, *J. Am. Chem. Soc.* **2024**, *146*, 22140−22144.

3.3. 铋催化的自由基型偶联反应

Josep Cornella (2023): **Bi**-radical catalysis in the activation of redox-active electrophiles (RAE)

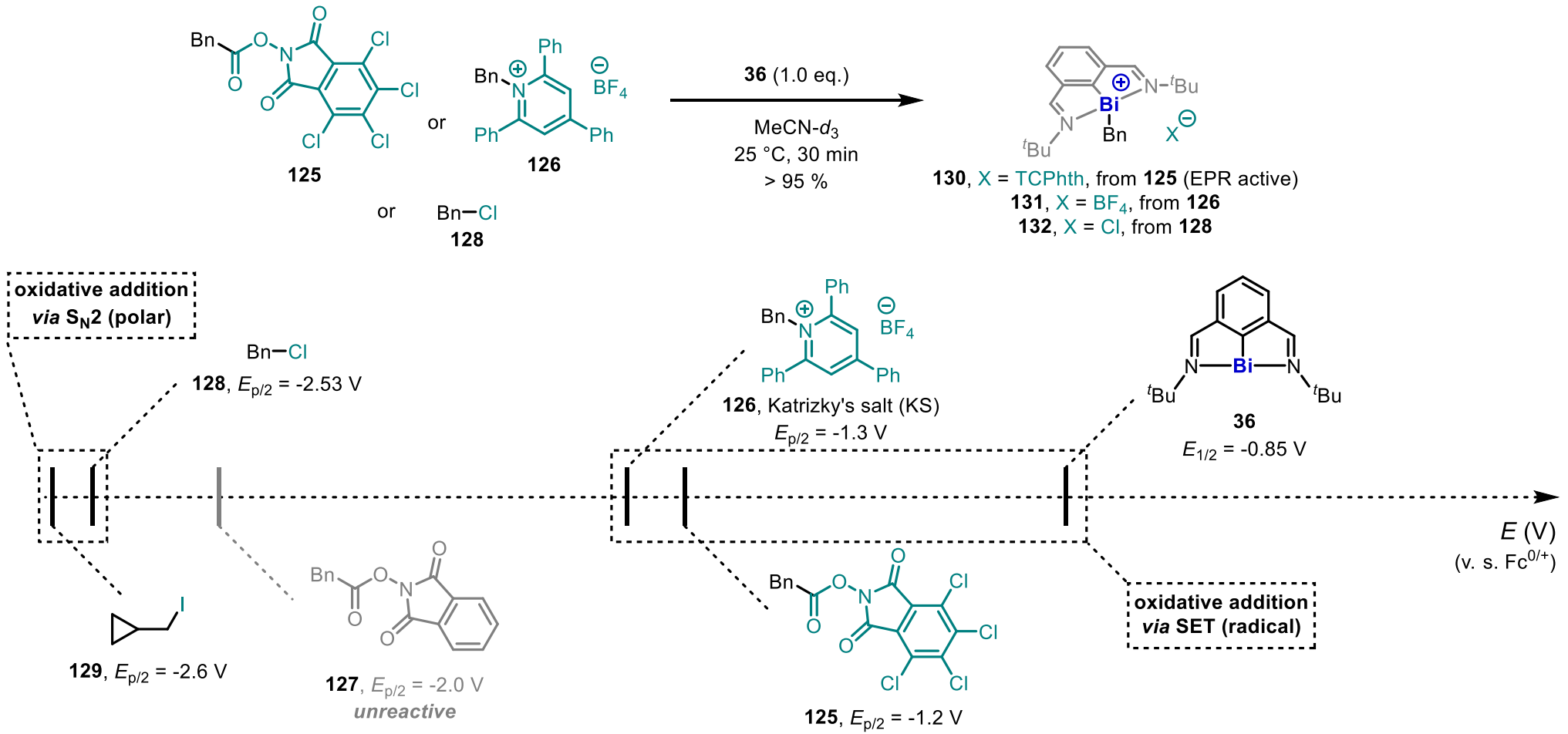

J. Cornella et al. *Nat. Chem.* **2023**, *15*, 1138-1145.

3.3. 铋催化的自由基型偶联反应

Josep Cornella (2023): **Bi**-radical catalysis in the activation of redox-active electrophiles (RAE)

Orthogonality to TM-mediated oxidative additions:

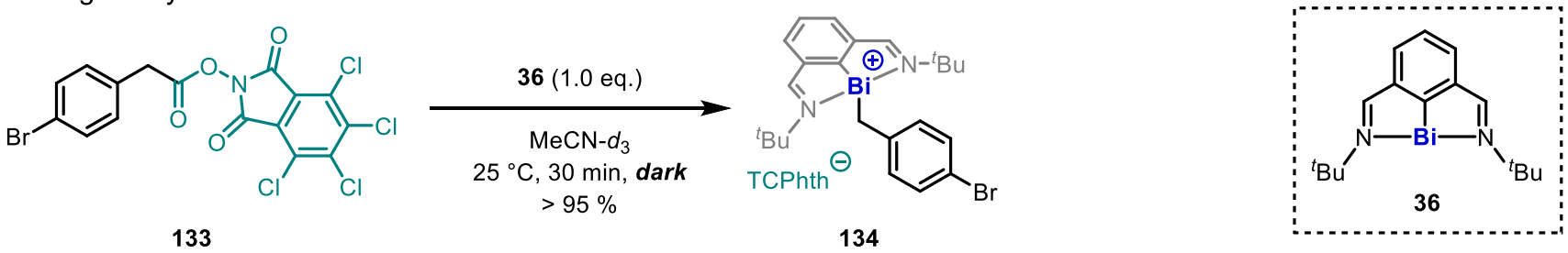

Evidence for alkyl-radical formattion after oxidative addition:

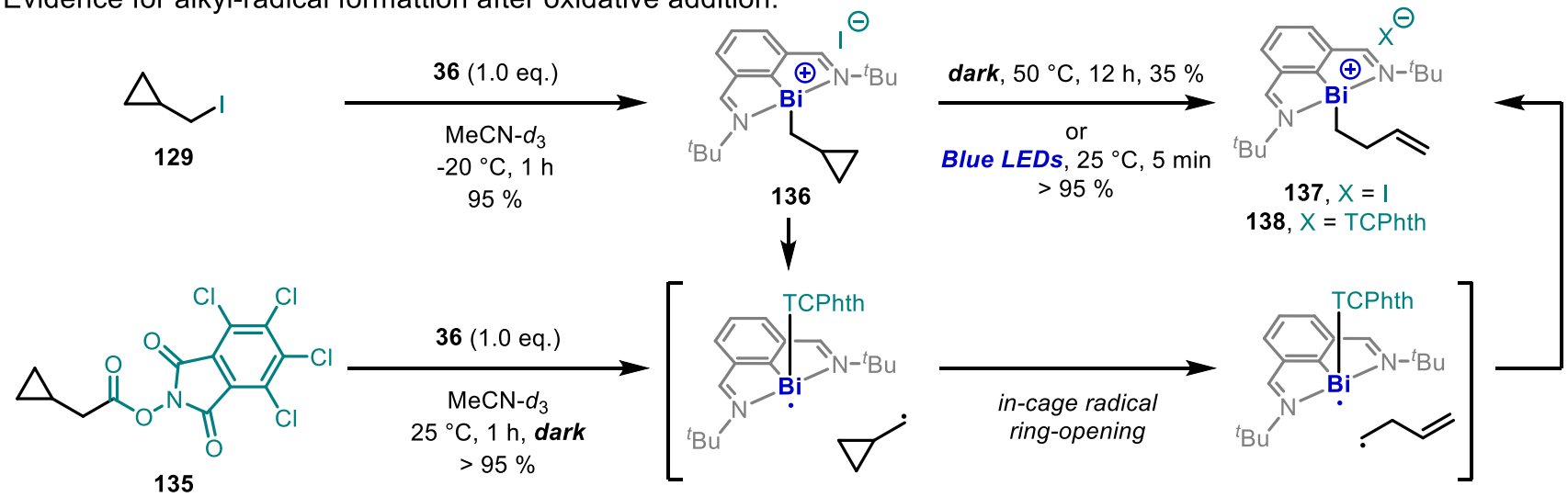

Alkyl radical could be formed both in the ***dark*** & under ***blue LEDs*** irridation;
blue LED could proceed radical formation & tolerate electrophiles other than RAEs

J. Cornella et al. *Nat. Chem.* **2023**, *15*, 1138-1145.

3.3. 铋催化的自由基型偶联反应

Josep Cornella (2023): **Bi**-radical catalysis in the activation of redox-active electrophiles (RAE)

Unbiased alkyl RAE v. s. α-amino alkyl RAE: **different reaction outcomes**

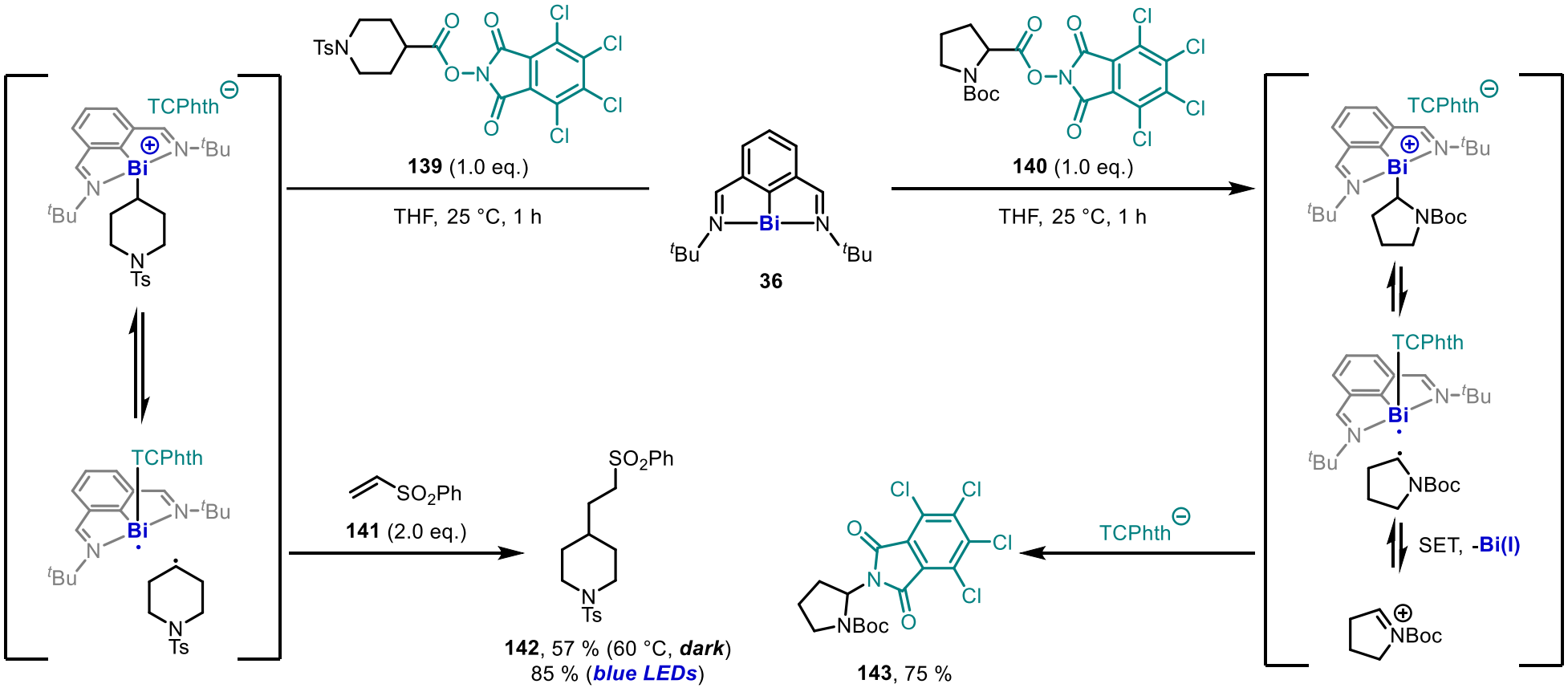

J. Cornella et al. *Nat. Chem.* **2023**, *15*, 1138-1145.

3.3. 铋催化的自由基型偶联反应

Josep Cornella (2023): **Bi**-radical catalysis in C(sp^3)-N coupling reaction

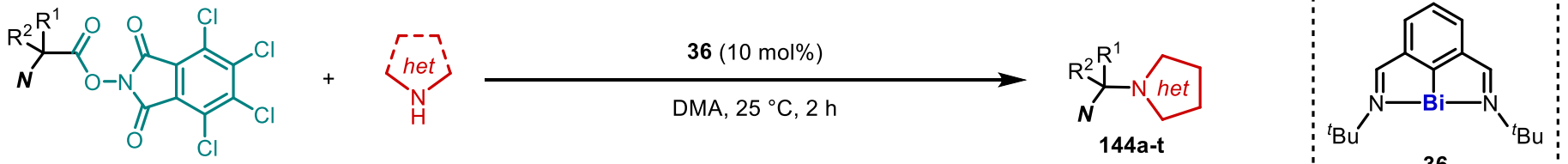

Scope of C(sp^3)-N coupling[a]

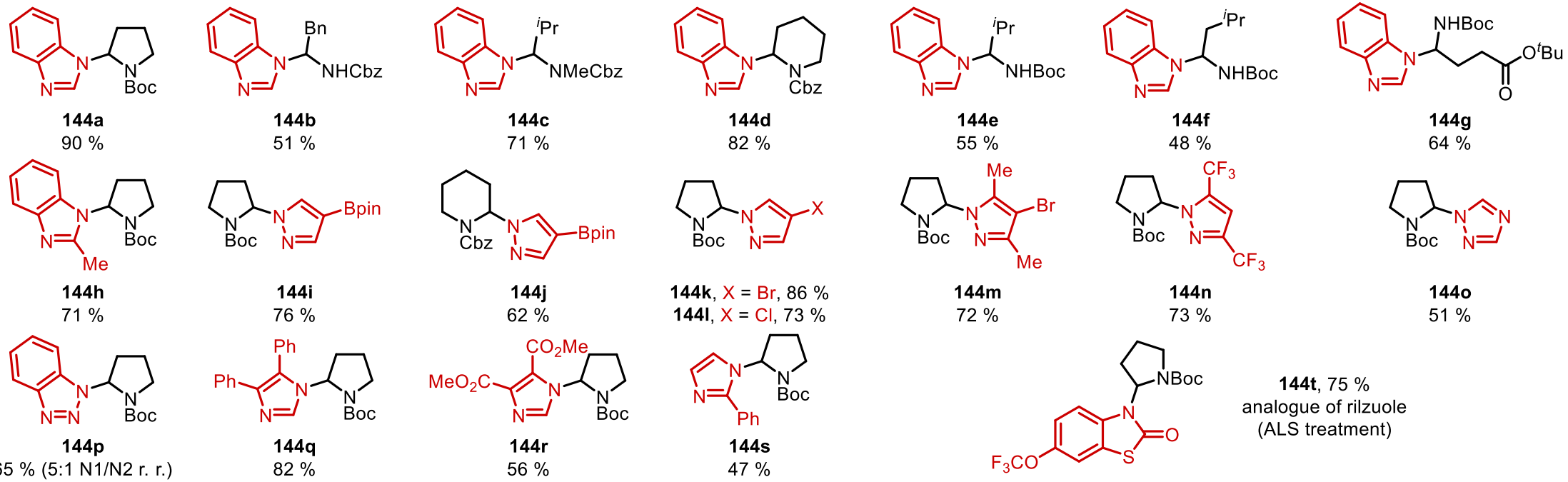

[a] Reaction conditions: RAE (0.2 mmol), *N*-nucleophile (3 eq.), **36** (10 mol %), DMA (0.033M) at 25 °C for 2 h; isolated yields.

J. Cornella et al. *Nat. Chem.* **2023**, *15*, 1138-1145.

3.3. 铋催化的自由基型偶联反应

Josep Cornella (2024): activation & C(sp^2)-C(sp^2) coupling of aryl iodides *via* **Bi**-photocatalysis

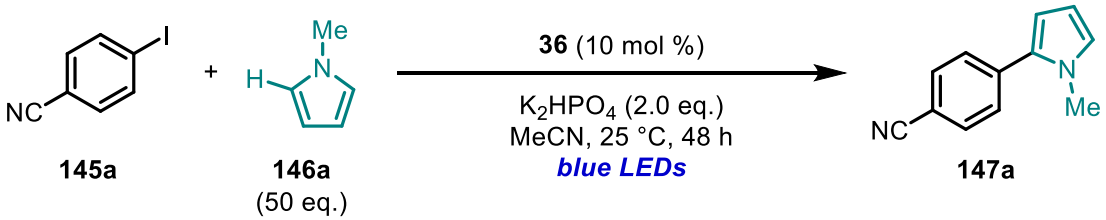

entry	deviations from above	NMR yield of **147a** (%)
1	none	58
2	w/o catalyst	< 1
3	w/o light, 45 °C	n. d.
4	w/o base	12
5	**35** or **124** instead of **36**	< 2

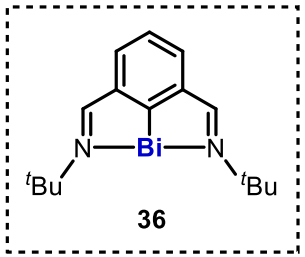

36

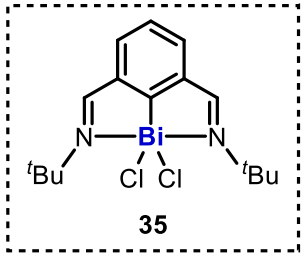

35

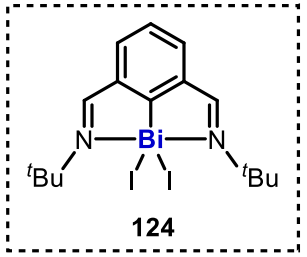

124

Selected scope of C(sp^2)-C(sp^2) cross coupling[a]

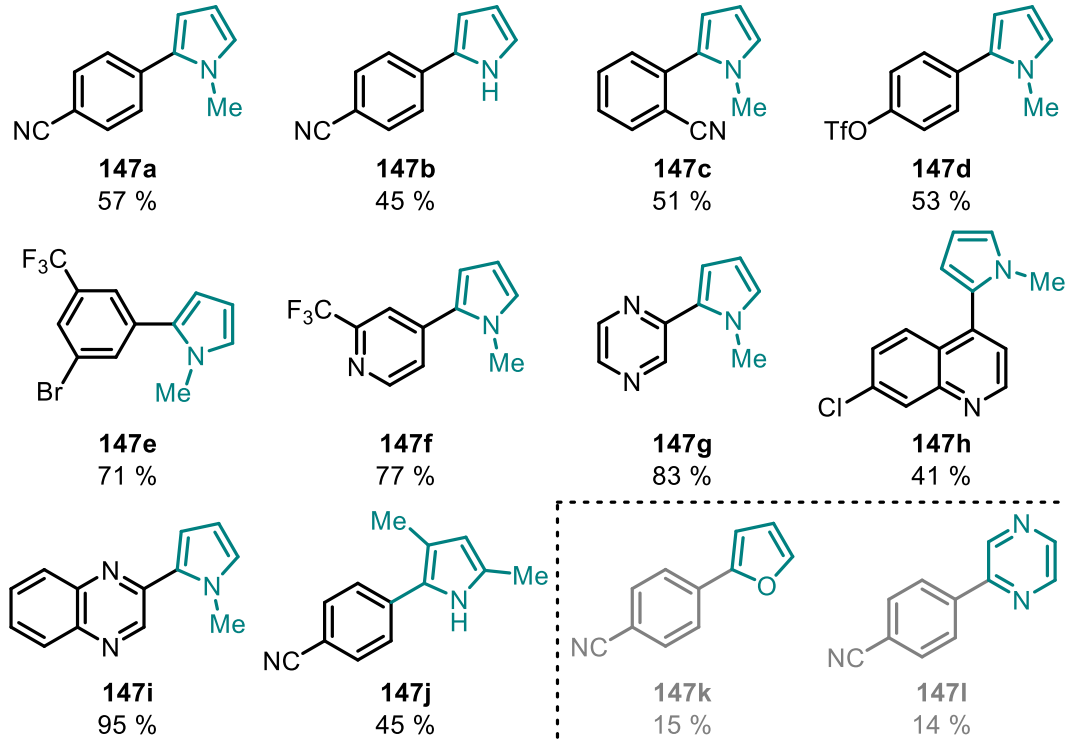

[a] Reaction conditions: aryl iodides (0.2 mmol), heterocycle nucleophile (50 eq.), K_2HPO_4 (2.0 eq.), **36** (10 mol %), MeCN (0.1 M) upon blue light irridiation (457 nm LED strip) at 25 °C for 60 h; isolated yield.

J. Cornella et al. *Angew. Chem. Int. Ed.* **2025**, *64*, e202418367.

3.3. 铋催化的自由基型偶联反应

Josep Cornella (2024): activation & C(sp^2)-C(sp^2) coupling of aryl iodides *via* **Bi**-photocatalysis

Counteranion-dependent photoreactivity of aryl-**Bi(III)** intermediates

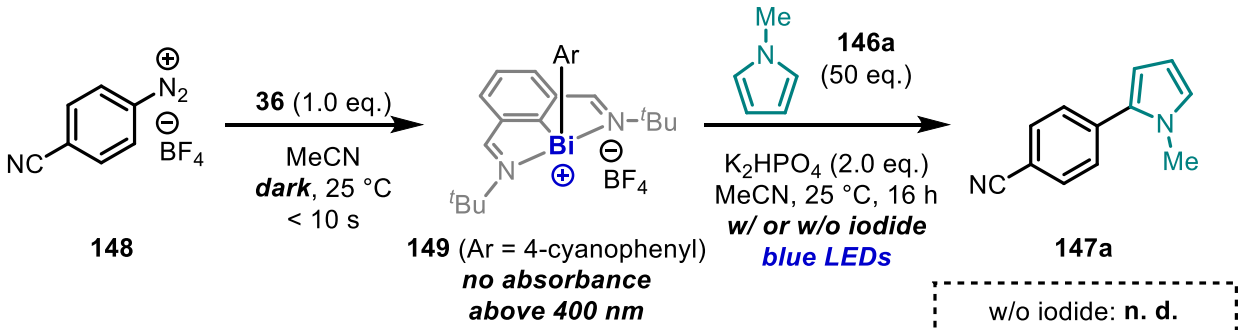

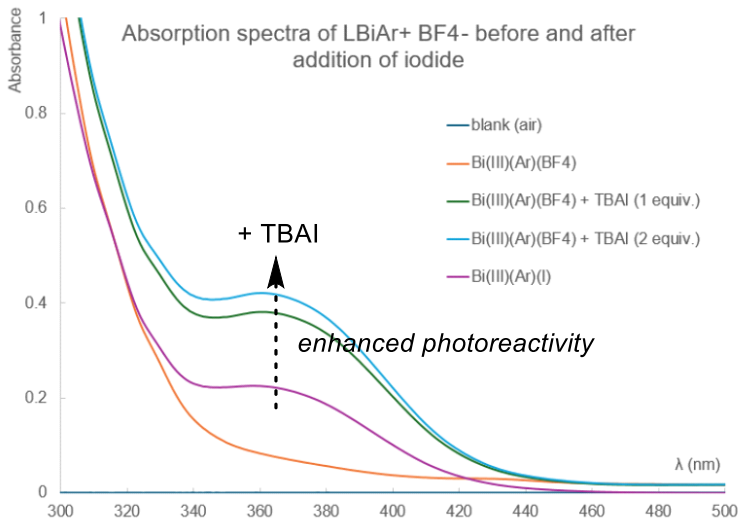

Possible mechanism (Ar = 4-cyanophenyl)

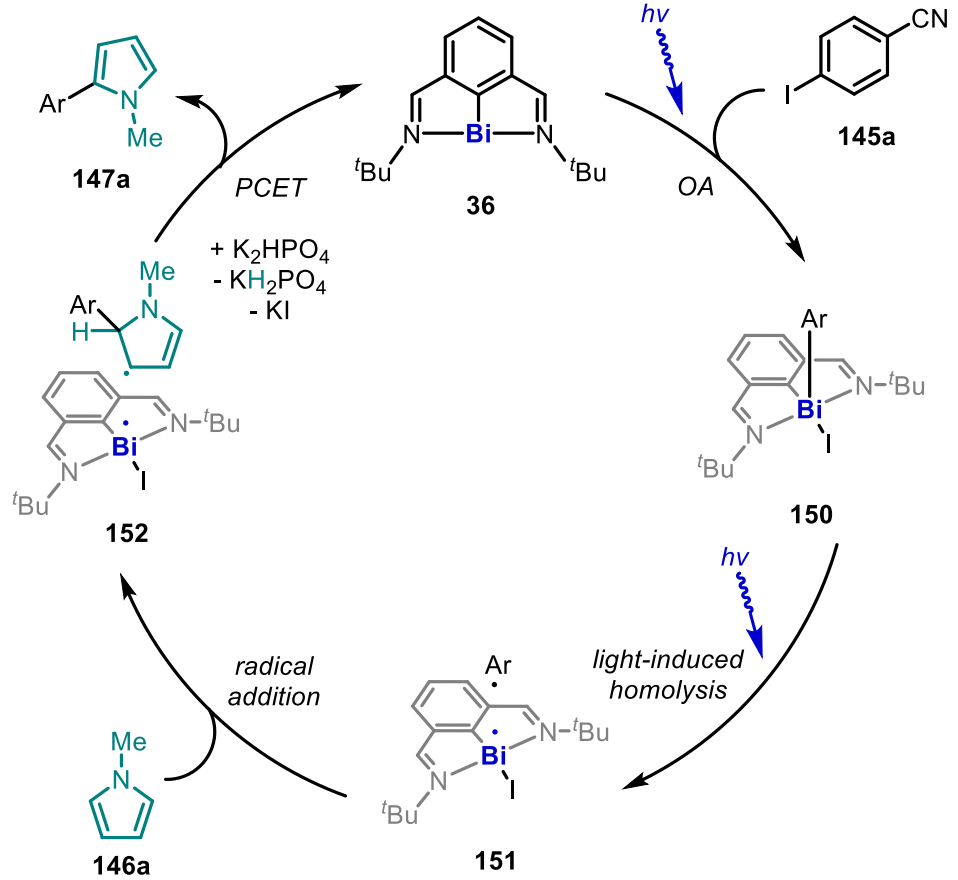

J. Cornella et al. *Angew. Chem. Int. Ed.* **2025**, *64*, e202418367.

3.3. 铋催化的自由基型偶联反应

Josep Cornella (2025): Heck-type C(sp^2)-C(sp^n) coupling *via* **Bi**-photocatalysis

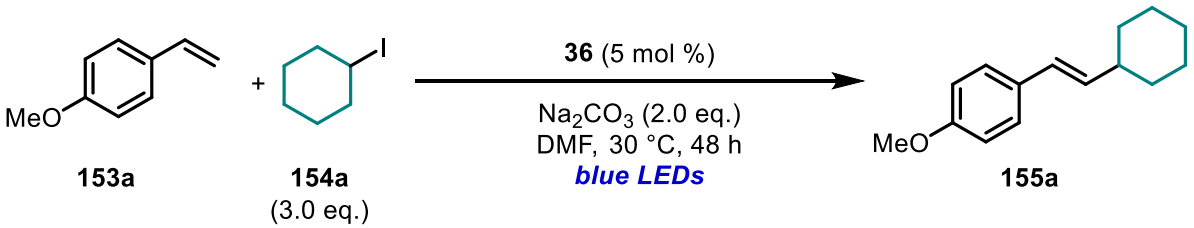

153a **154a** (3.0 eq.) **155a**

entry	deviations from above	NMR yield of **155a** (%)
1	none	85
2	w/o catalyst	0
3	w/o light	0
4	w/o base	19
5	**35** or **124** instead of **36**	81

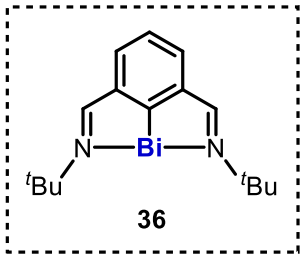

36

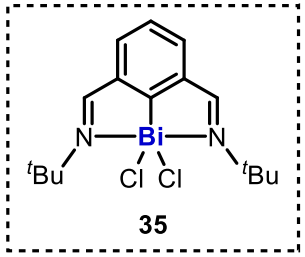

35

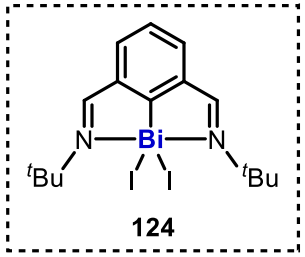

124

Selected scope of Heck-type C(sp^2)-C(sp^3) coupling[a]

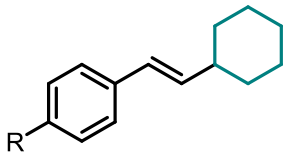

155a, R = OMe, 81 %
155b, R = F, 72 %[b][c]
155c, R = Cl, 61 %[b][c]
155d, R = Bpin, 39 %[b][d]

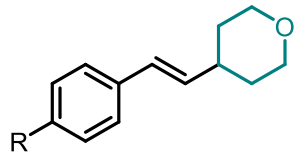

155e, R = Ph, 42 %[c]
155f, R = SMe, 57 %
155g, R = OMe, 69 %
155h, R = Br, 59 %[b][c]

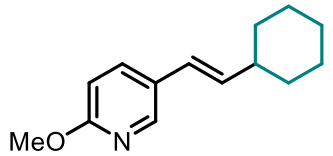

155i, 65 %

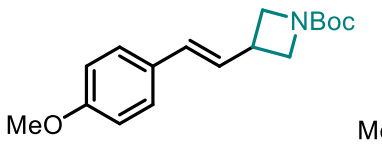

155j, 47 %

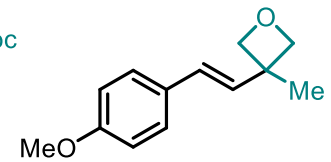

155k, 51 %

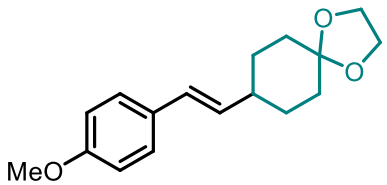

155l, 87 %

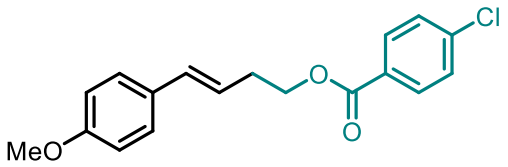

155m, 77 %[c]

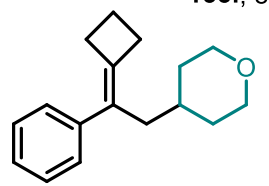

155n, 86%

[a] Reaction conditions: styrenes (1.0 eq.), alkyl iodides (3.0 eq.), Na_2CO_3 (2.0 eq.), **36** (5 mol %), DMF (0.1 M) upon blue light irridiation (456 nm LED strip) at 30 °C for 48 h; isolated yield; the products have a *E*/*Z* ratio of >15:1 unless otherwise specified; [b] 390 nm LEDs; [c] *E*/*Z* = 10:1.

J. Cornella et al. *Nat. Catal.* **2025**, https://doi.org/10.1038/s41929-025-01438-y.

3.3. 铋催化的自由基型偶联反应

Josep Cornella (2025): Heck-type C(sp^2)-C(sp^n) coupling *via* **Bi**-photocatalysis

Selected scope of Heck-type C(sp^2)-C(sp^2) coupling[a]

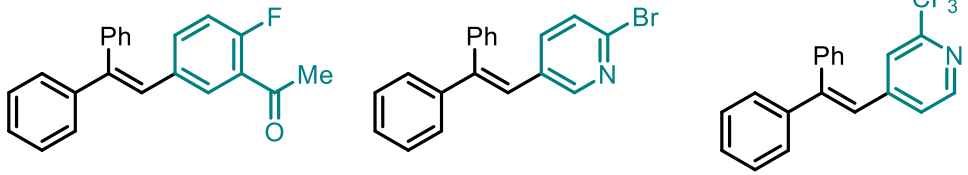

155o, 56 %

155p, 51 %

155q, 37 %

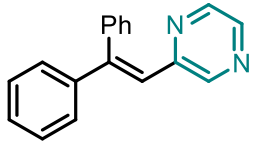

155r, 88 %

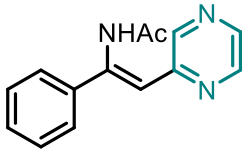

155s, 43 %

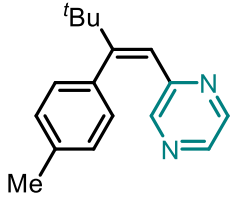

155t, 53 %

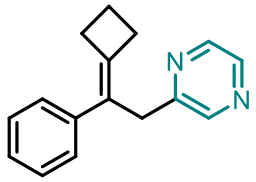

155u, 71 %

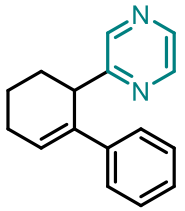

155v, 53 %

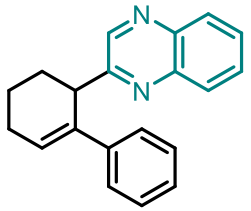

155w, 36 %

[a] Reaction conditions: styrenes (3.0 eq.), aryl iodides (1.0 eq.), Na_2CO_3 (2.0 eq.), **36** (5 mol %), DMF (0.1 M) upon blue light irridiation (456 nm LED strip) at 30 °C for 48 h; isolated yield; the products have a *E*/*Z* ratio of >15:1 unless otherwise specified.

Radical clock experiment

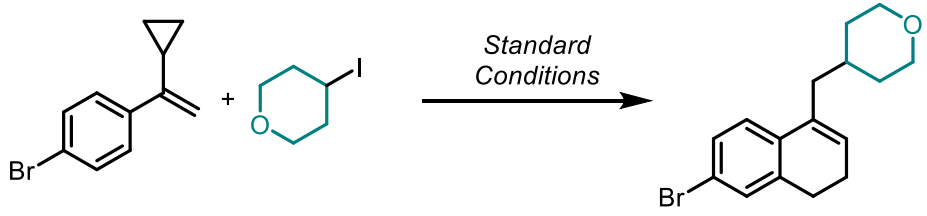

156 **157** **158**, 36 %

Probe for feasibility of radical-polar crossover (RPC)

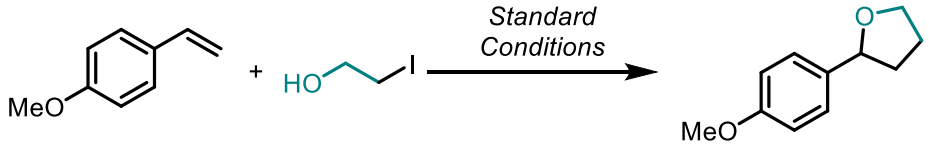

153a **159** **160**, 54 %

Different mechanism for aryl and alkyl electrophiles

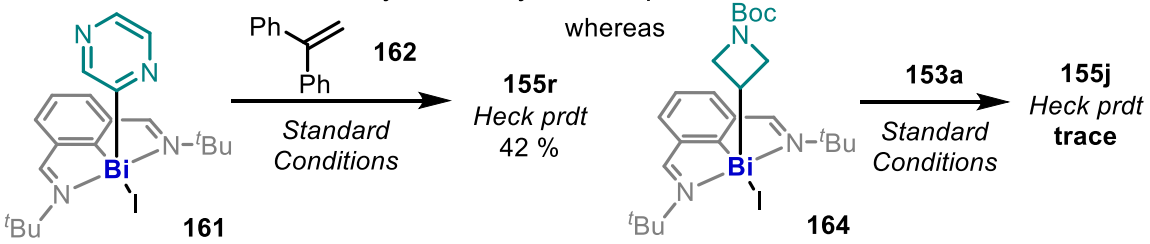

161 **164**

J. Cornella et al. *Nat. Catal.* **2025**, https://doi.org/10.1038/s41929-025-01438-y.

3.3. 铋催化的自由基型偶联反应

Josep Cornella (2025): Heck-type C(sp^2)-C(sp^n) coupling *via* **Bi**-photocatalysis

Stoichiometric radical clock experiment to probe for reversible, **Bi**-mediated C-centered radical formation

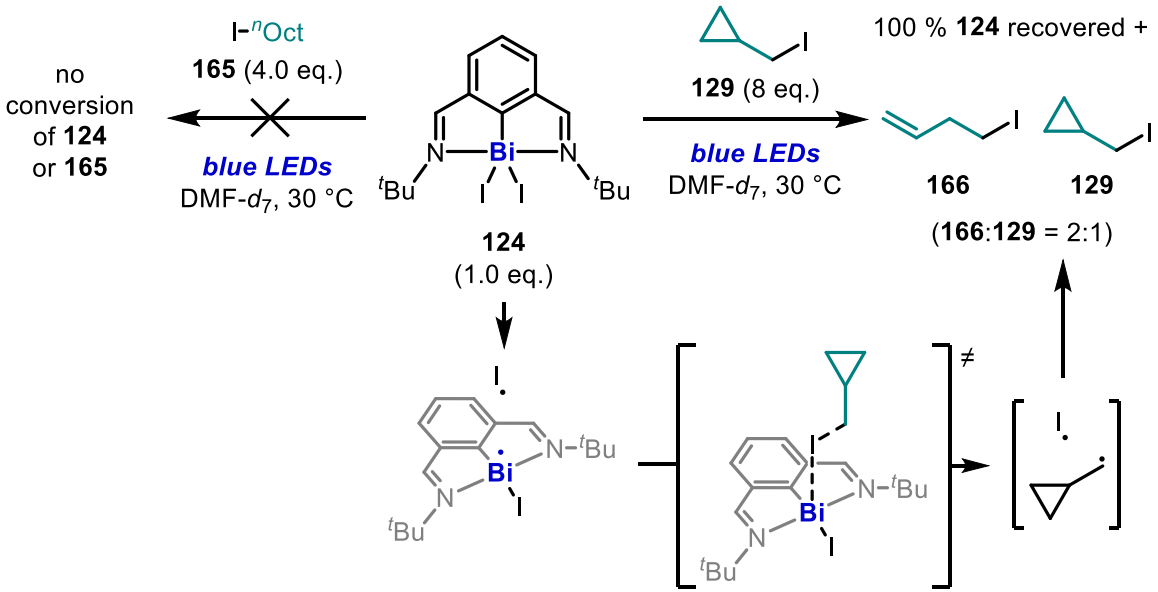

J. Cornella et al. *Nat. Catal.* **2025**, https://doi.org/10.1038/s41929-025-01438-y.

3.3. 铋催化的自由基型偶联反应

Josep Cornella (2025): Heck-type C(sp^2)-C(sp^n) coupling *via* **Bi**-photocatalysis

Stoichiometric radical clock experiment to probe for reversible, **Bi**-mediated C-centered radical formation

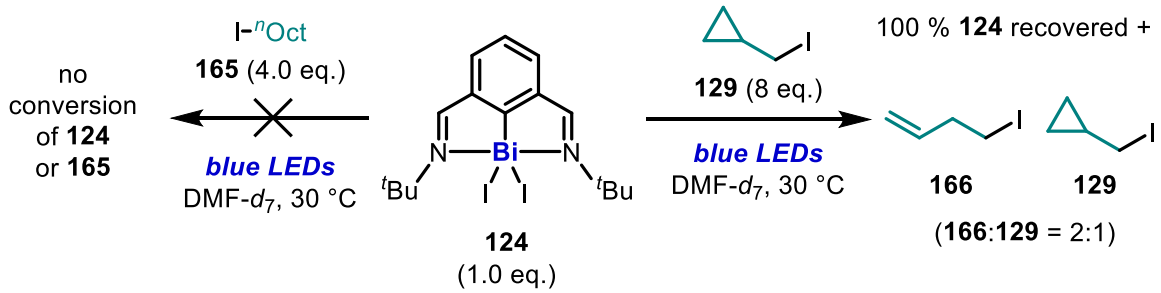

Stoichiometric radical clock experiment to probe for **XAT** between nascent **Bi(II)** & alkyl iodides

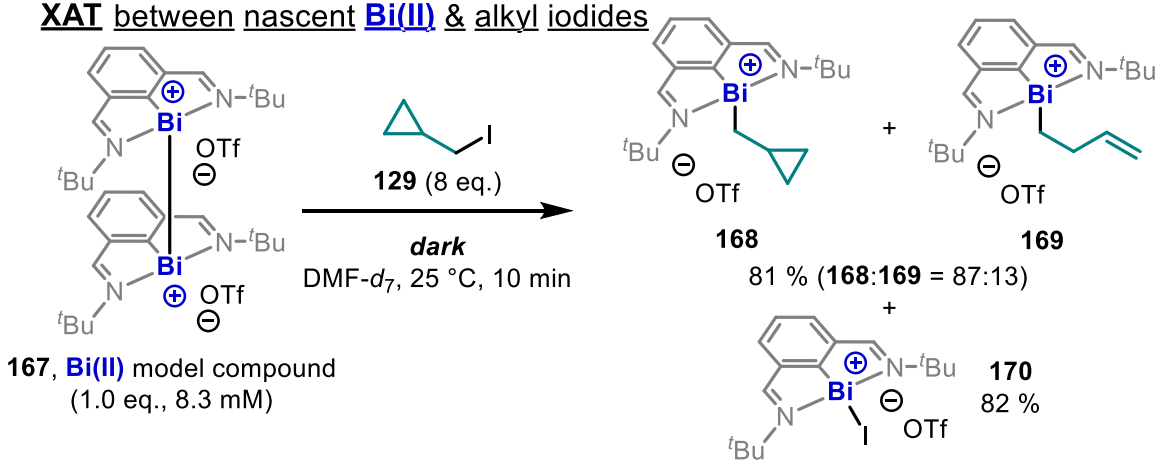

167, **Bi(II)** model compound
(1.0 eq., 8.3 mM)

J. Cornella et al. *Nat. Catal.* **2025**, https://doi.org/10.1038/s41929-025-01438-y.

3.3. 铋催化的自由基型偶联反应

Josep Cornella (2025): Heck-type C(sp^2)-C(sp^n) coupling *via* **Bi**-photocatalysis

Stoichiometric radical clock experiment to probe for reversible, **Bi**-mediated C-centered radical formation

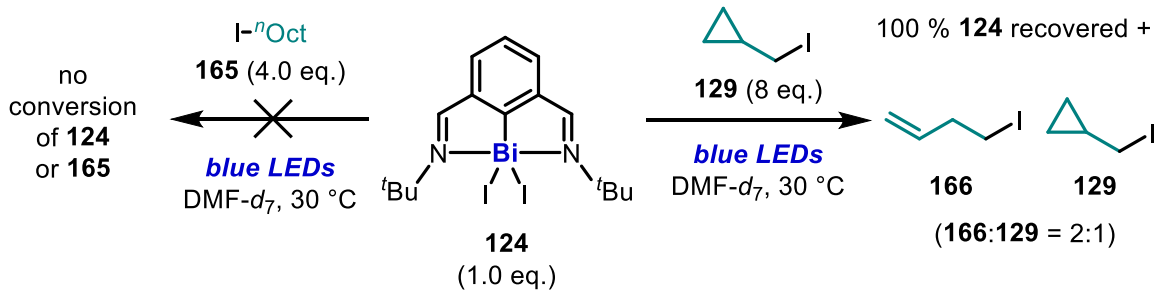

Stoichiometric radical clock experiment to probe for **XAT** between nascent **Bi(II)** & alkyl iodides

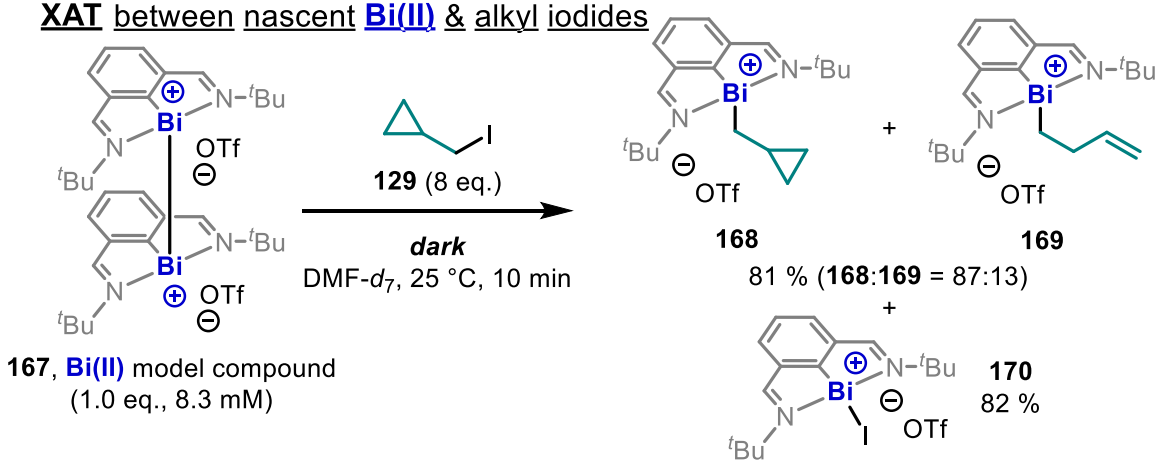

Mechanism for Heck-type C(sp^2)-C(***sp*²**) coupling

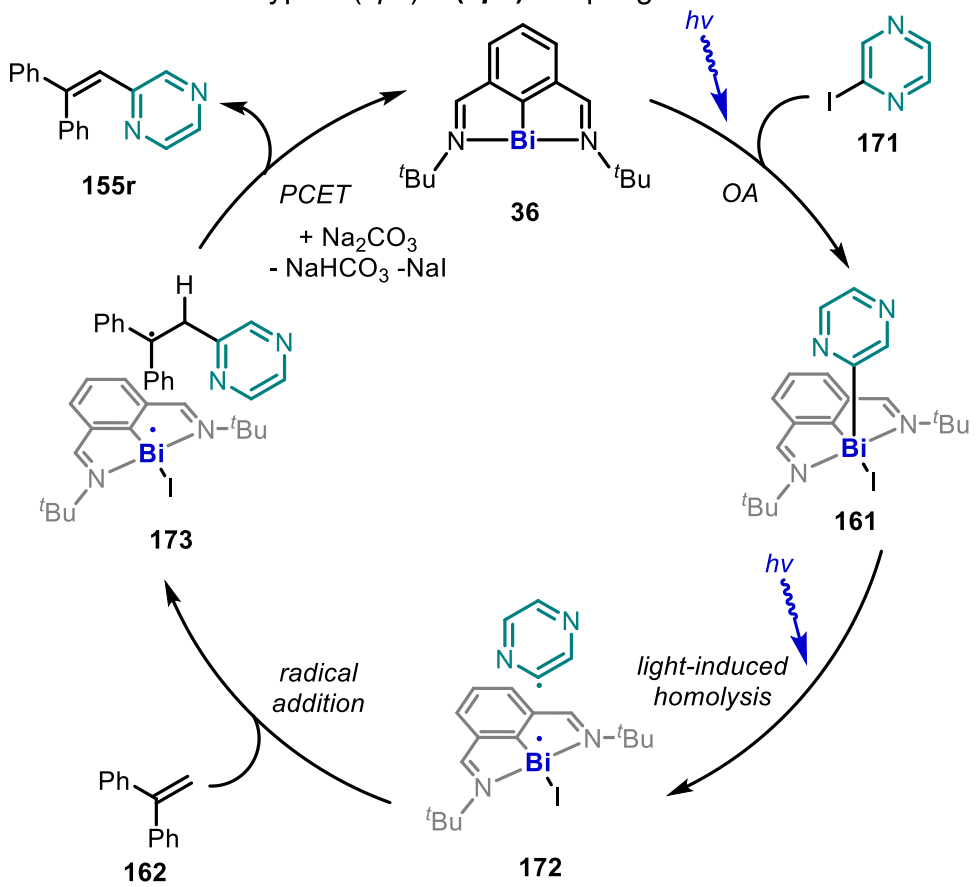

J. Cornella et al. *Nat. Catal.* **2025**, https://doi.org/10.1038/s41929-025-01438-y.

3.3. 铋催化的自由基型偶联反应

Josep Cornella (2025): Heck-type C(sp^2)-C(sp^n) coupling *via* **Bi**-photocatalysis

Stoichiometric radical clock experiment to probe for reversible, **Bi**-mediated C-centered radical formation

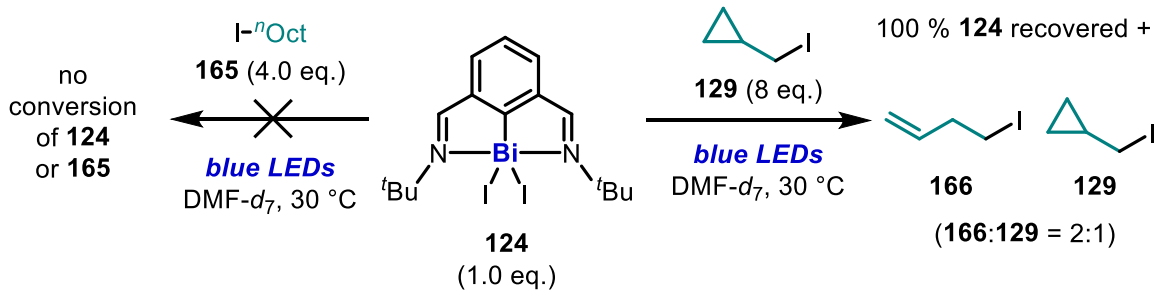

Stoichiometric radical clock experiment to probe for **XAT** between nascent **Bi(II)** & alkyl iodides

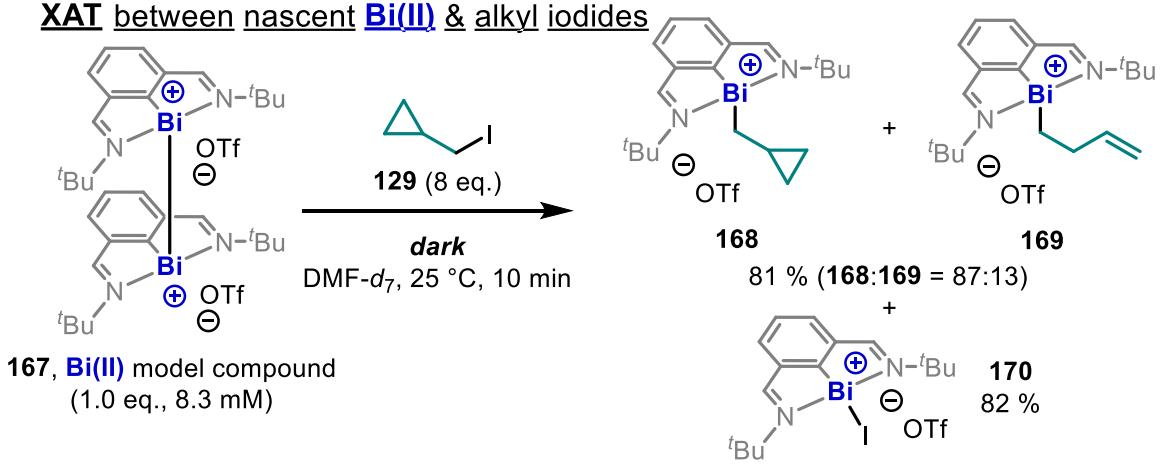

Mechanism for Heck-type C(sp^2)-C(***sp*^{3}**) coupling

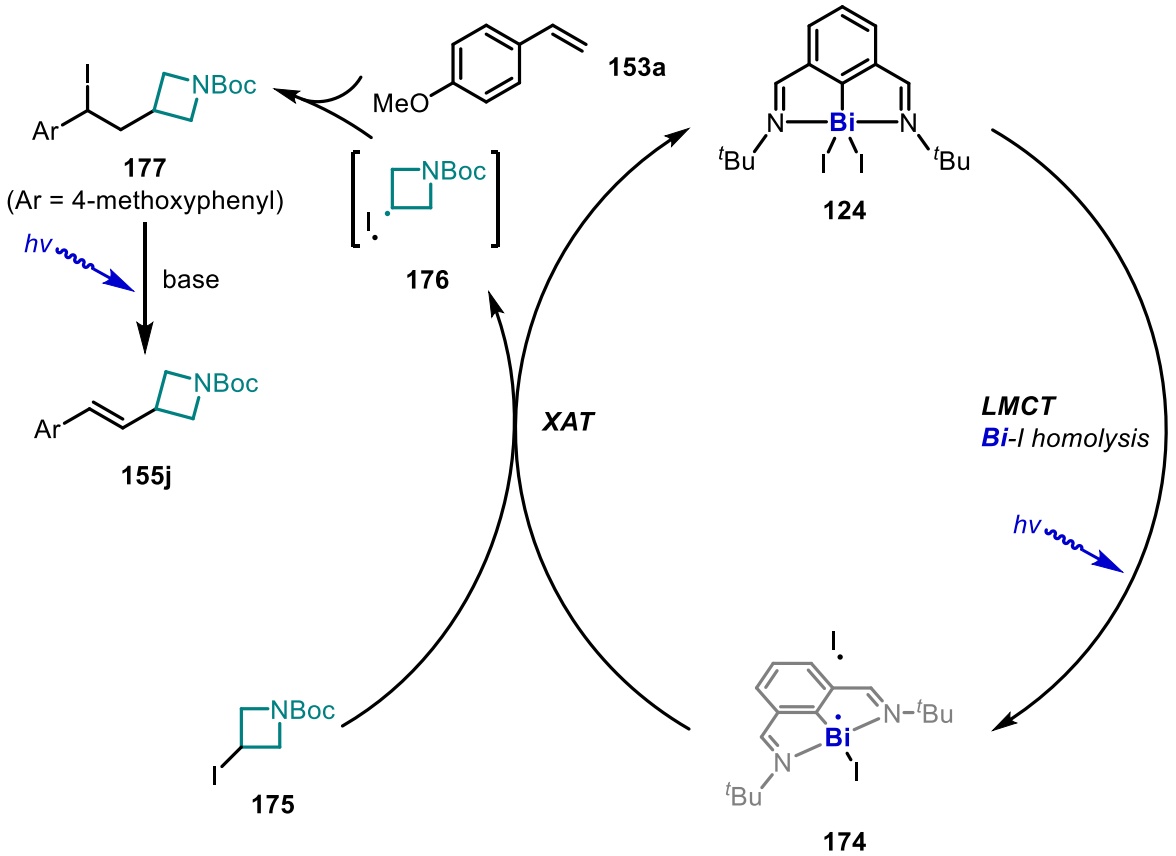

J. Cornella et al. *Nat. Catal.* **2025**, https://doi.org/10.1038/s41929-025-01438-y.

目录

4. 总结与展望

Summary

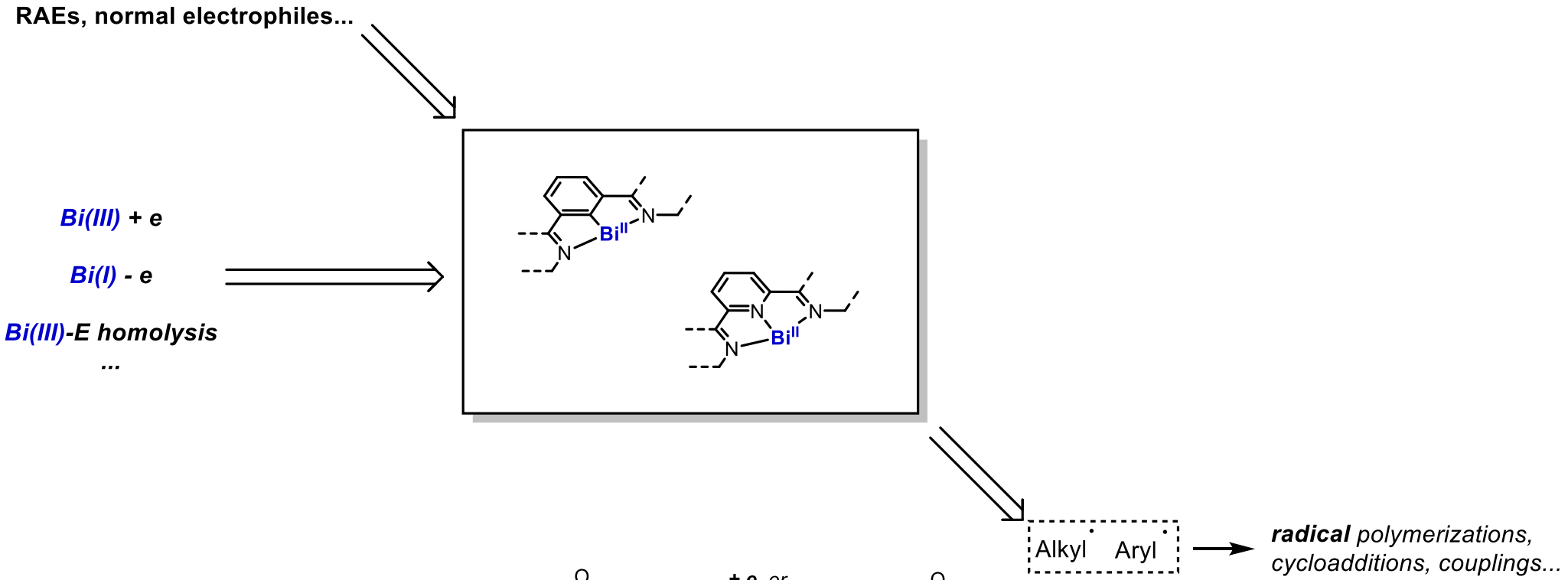

Challenges:

1) Characterization or isolation of elusive **Bi(IV)** radicals;

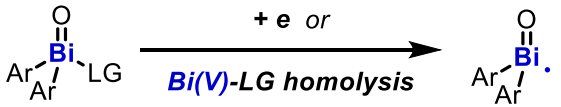

2) Exploration of **bismuthinidenes** on small molecule activation.

For a detailed summary of bismuth in radical chemistry & catalysis, see: M. Mato, J. Cornella, *Angew. Chem. Int. Ed.* **2024**, *63*, e202315046.

Thanks for your kind attention!

2025年11月21日